CHEMISTRY AND CATALYSIS OF COAL LIQUEFACTION; CATALYTIC AND THERMAL UPGRADING OF COAL LIQUIDS; AND HYDROGENATION OF CO TO PRODUCE FUELS. VOLUME 7. FINAL REPORT

UTAH UNIV., SALT LAKE CITY. DEPT. OF FUELS ENGIEERING

15 JUN 1985

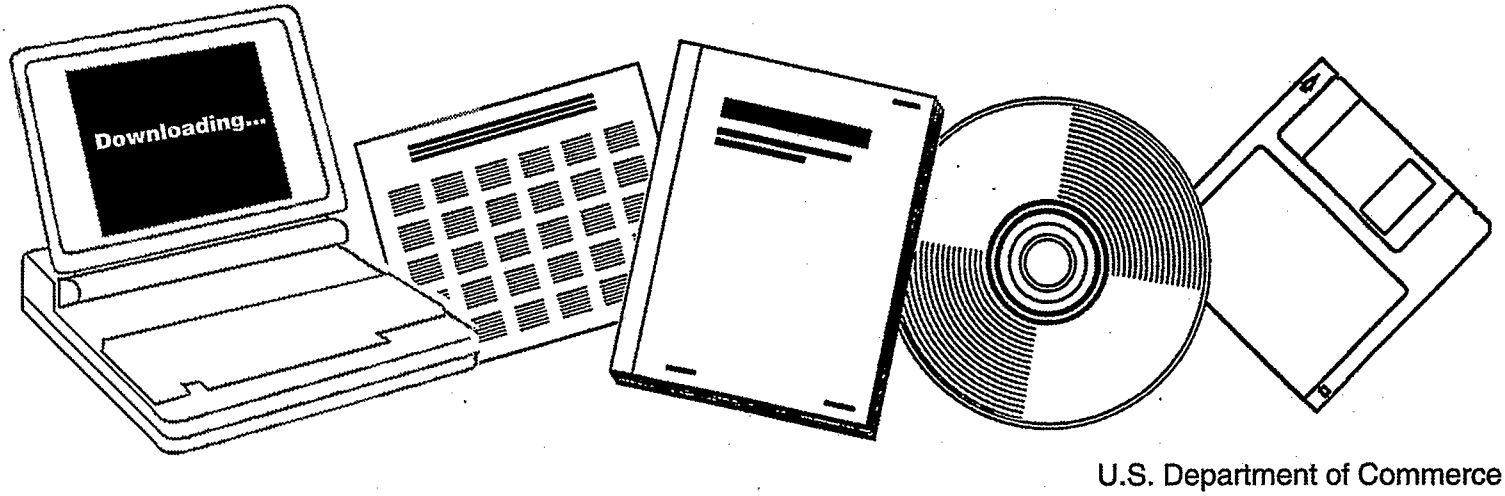

DOE/ET/14700--T1-Vol.7

DE85 014171

ABSTRACT

A series of Raney iron (Fe) and Raney iron-manganese (Fe-Mn) catalysts have been investigated for application to the hydrogenation of carbon monoxide for the production of low molecular weight olefins (C_2-C_4).

The Raney Fe and Raney Fe-Mn catalysts were prepared by leaching the aluminum from Al-Fe (50/50 weight percent, wt %) and Al-Fe-Mn (59/38/3 wt %) alloys with an aqueous solution of sodium hydroxide. The variables investigated in the catalyst preparation and activation studies included leaching temperature (298 - 363 K), NaOH concentration (2 to 20 wt %), and leaching mode (alloy addition or caustic addition). The extent of aluminum leaching was determined by the evolution of hydrogen gas during the leaching process:

$$2\ NaOH + 2\ Al + 2\ H_2O = 2\ NaAlO_2 + 3\ H_2 \uparrow .$$

The extent of aluminum leaching increased with increasing leaching temperature and increasing sodium hydroxide concentration, irrespective of leaching mode.

The Raney catalysts were characterized by x-ray diffraction and BET surface area measurements. The major phase in all the Raney Fe and Raney Fe-Mn catalysts was α-Fe. Magnetite was found in the catalysts activated at the high leaching temperature (363 K), whereas unreacted aluminum alloy phases were found in the catalysts

CONTENTS

prepared at a low leaching temperature (298 K). The BET surface area of the Raney Fe catalysts varied from 26 to 54 m^2/g, while the BET surface area of Raney Fe-Mn varied from 64 to 116 m^2/g depending on the preparation conditions.

The crystallite size of the α-Fe in the Raney catalysts was estimated by x-ray line broadening and ranged from 70 to 250 Å. The crystallite size increased with increasing leaching temperature. A linear relationship existed between the surface area and the reciprocal of the crystallite size.

Thermogravimetric analyses have been carried out to determine the optimum reduction conditions for both the Raney and precipitated iron and the Raney and coprecipitated iron-manganese catalysts. The optimum reduction temperature was 648 K for the Raney catalysts and was 673 K for the precipitated catalysts. Both types of catalyst underwent essentially complete reduction in flowing H_2 within 5 hours at the above reduction temperatures.

The Raney and precipitated catalysts, reduced in-situ in flowing hydrogen, were evaluated in a high pressure fixed-bed reactor to assess catalytic activity and selectivity for the hydrogenation of carbon monoxide at the following standard reaction conditions: pressure = 1465 KPa (200 psig), space velocity = 3.0 $cm^3g^{-1}s^{-1}$, H_2/CO = 2.0, and reaction temperature of 423 to 473 K.

The catalytic activity of the Raney catalysts (Fe and Fe-Mn), as measured in terms of carbon monoxide conversion, generally increased with increasing leaching temperature for each mode of preparation. The Raney Fe and Raney Fe-Mn catalysts were 2 to 4 times

more active than the corresponding precipitated Fe and Fe-Mn catalysts, respectively, at the standard reaction conditions. The activation energy ranged from 96 to 139 KJ/mol depending on different catalysts.

The C_2-C_4 hydrocarbon yields for the Raney Fe and the Raney Fe-Mn catalysts were similar, ranging from 34 to 40 percent at 453 K. However, the Raney Fe-Mn catalysts showed higher C_2-C_4 olefin selectivity than the Raney Fe catalysts. The same trend was found for the precipitated Fe and coprecipitated Fe-Mn catalysts. Less than 7 wt % Mn in the coprecipitated Fe-Mn and in the Raney Fe-Mn catalysts increased the olefin selectivity of the catalyst by a factor of about two.

The Hydrogenation of Carbon Monoxide over Raney Iron-Manganese Catalysts

Francis V. Hanson
Alex G. Oblad

Introduction

The Fischer-Tropsch process, commercialized in Germany in the 1930s, was developed mainly to produce gasoline-boiling range hydrocarbons from carbon monoxide and hydrogen over metal catalysts such as iron, nickel, and cobalt. This process is quite flexible in that a wide spectrum of hydrocarbons such as gasoline, fuel oil, alcohols, and high molecular weight waxes can be produced by using an appropriate catalyst and by adjusting the process operating conditions.

After the Second World War and until recently, this process did not attract widespread interest in the United States due to the relative abundance of low cost petroleum resources. Today the only commercial Fischer-Tropsch plant in service in the world is at Sasolburg in South Africa. However, the recent paucity of reliable petroleum supplies, especially after the 1973 oil embargo, led to a resurgence of interest in development efforts on alternative fossil energy resources such as coal, heavy oil, shale oil, and tar sands. The prime objective of these investigations was to develop technology for the production of liquid fuels from these resources.

A serious imbalance in the demand and supply of chemical feedstocks for the chemical process industries is expected in the near future. This is especially true with regard to low molecular weight

hydrocarbons such as ethylene, propylene, and butenes which are among the most important feedstocks.[1]

Recently, a number of active catalyst research and development programs have been initiated to explore the potential of carbon monoxide hydrogenation as a source of light olefins.

The selective production of low molecular weight olefins and oxygenated compounds from carbon monoxide and hydrogen at elevated temperatures and pressures has been reported[2,3] for iron and cobalt catalysts, for iron-manganese catalysts, and for metal catalysts promoted with vanadium, manganese, and chromium. An iron-manganese catalyst (Mn/Fe atomic ratio 9/1) was claimed to be extremely selective for the production of low molecular weight olefins at a reactor temperature of 553 K, a reactor pressure of 1465 KPa, a hydrogen-to-carbon monoxide ratio of 0.71, and a space velocity of 340 GHSV.[2,3] The olefin-to-paraffin ratio for the low molecular weight hydrocarbon (C_2-C_4) fraction was 2.3 to 1 at a conversion (H_2 + CO) of 76 percent. Yang and co-workers[4-7] conducted an extensive catalyst screening program to determine the activity and selectivity of a wide variety of catalysts for the production of low molecular weight (C_2-C_4) olefins. The screening included unsupported and supported catalysts and promoted and unpromoted catalysts. The most promising catalyst system to emerge from these studies was the iron-manganese series of catalysts. An extensive process variable investigation with the coprecipitated iron-manganese catalysts has been carried out by Tsai and co-workers.[8,9] The process variables studied included reactor temperature, reactor pressure, reactant space velocity, and hydrogen-to-carbon monoxide ratio. The catalyst

compositions ranged from an atomic ratio of 1.1 Mn/100 Fe to an atomic ratio of 607 Mn/100 Fe. The most selective catalysts had manganese-to-iron atomic ratios in the range of 2 Mn/100 Fe to 60 Mn/100 Fe, that is, the C_2-C_4 hydrocarbon yield was 50 mole percent of which 75 percent was olefinic. Above an atomic ratio of 70 Mn/100 Fe the olefin-to-paraffin ratio declined significantly at the standard operating conditions.

A variety of other metal catalysts have been evaluated for the synthesis of low molecular weight hydrocarbons from hydrogen and carbon monoxide, that is, cobalt,[10] nickel,[11] rhodium,[12] and molybdenum.[13] However, the selectivities of these catalysts for C_2-C_4 olefins were much lower than that reported for coprecipitated iron-manganese catalysts.[2,3]

Raney metal catalysts have been successfully used as hydrogenation catalysts in the synthesis of a variety of chemicals, however, little has been reported in the literature regarding their application in Fischer-Tropsch type synthesis. The only exceptions involve methanation studies.[14-17] A Raney nickel catalyst was found to be far more active than any of the conventional nickel catalysts investigated for methanation applications in fixed-bed and fluid-bed reactors.[17]

The objective of this investigation was to assess the potential of Raney iron and Raney iron-manganese catalysts for the production of low molecular weight olefins from hydrogen and carbon monoxide at commercially feasible process operating conditions. The main focus of the experimental program was the preparation,

characterization, and evaluation of the Raney iron and Raney iron-manganese catalysts.

EXPERIMENTAL METHODS AND MEANS

Alloy Preparation

Electric Heating Furnace

An electric heating furnace was built to prepare the Al-Fe and the Al-Fe-Mn alloys. A schematic of the furnace is presented in Figure 10 and detailed drawings of the furnace design are included in Appendix A.

The furnace consisted of six Kanthal Super 33 heating elements, a mullite tube, and a copper sealing and cooling unit. The temperature of the furnace was controlled by a SCR power controller (Research Incorporated, Model 64600) and a temperature controller (Research Incorporated, Model 61011). An S-type thermocouple was positioned just above the alloy sample to control the temperature. Another S-type thermocouple was installed near the heating element in the hot box to prevent overheating the furnace.

The dimensions of the hot box were determined based on the maximum amount of the alloy sample desired from each batch. The number of heating elements was determined based on the hot box size-power input relationship obtained from the Kanthal Handbook.[152] The dimensions and positions of other parts, such as a mullite tube and a copper sealing unit, were determined according to the dimension of the hot box.

Figure 10

Schematic of Electric Heating Furnace

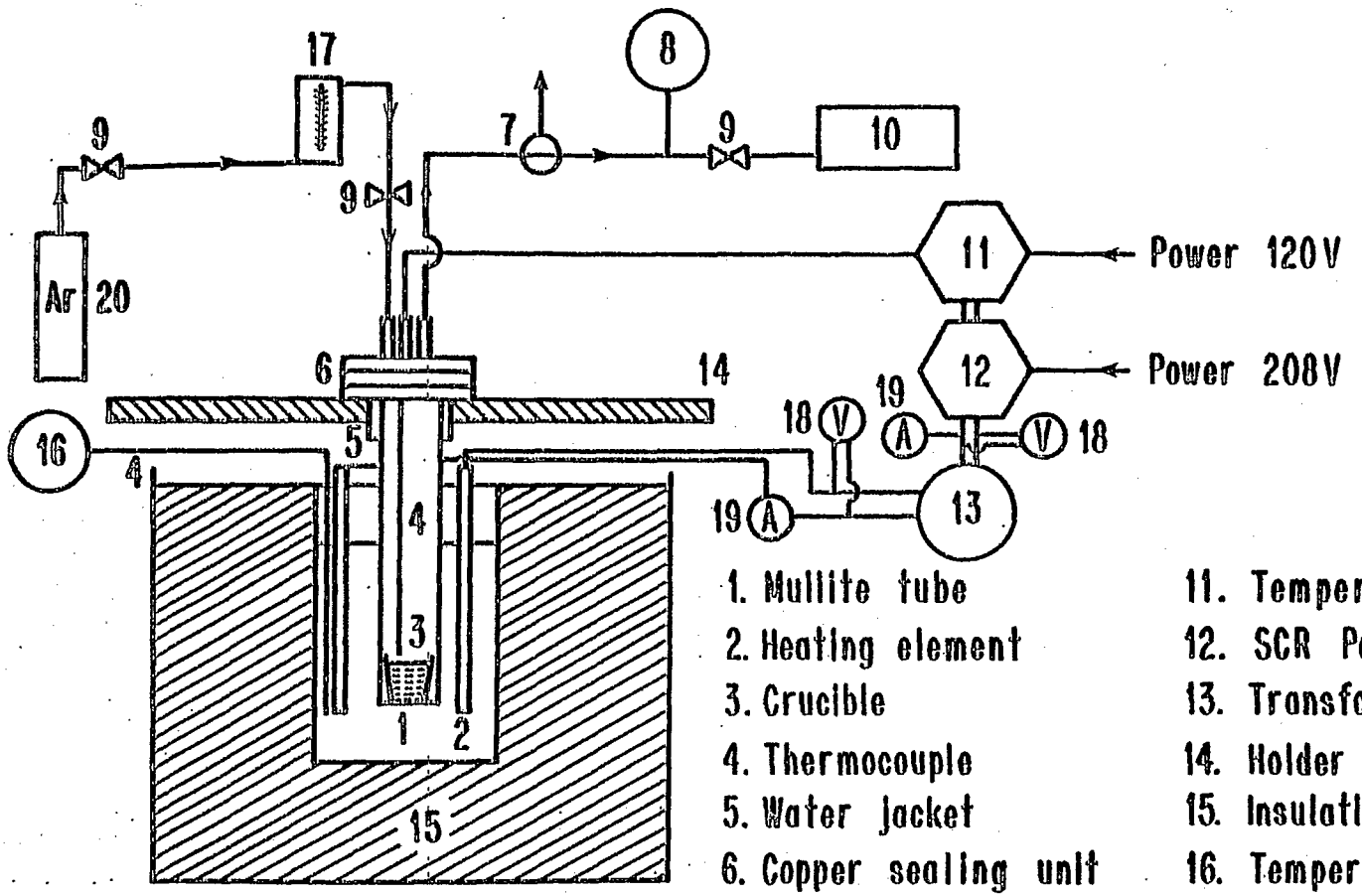

1. Mullite tube
2. Heating element
3. Crucible
4. Thermocouple
5. Water jacket
6. Copper sealing unit
7. 3-Way valve
8. Vacuum gauge
9. On-off valve
10. Vacuum pump
11. Temperature controller
12. SCR Power controller
13. Transformer
14. Holder
15. Insulating brick
16. Temperature indicator
17. Rotameter
18. Voltmeter
19. Ammeter
20. Argon gas cylinder

The power source for the furnace was 208 volt x 30 ampere AC. The voltage of the incoming power to the transformer (Matra Electric, Inc., single phase 2 wire output) was stepped down 4 to 1 to obtain a high electric current in the heating elements. The maximum electric current in the heating elements was limited to 150 amperes to protect the elements from overloading.

The mullite tube was a cylinder with one end open, 3.75 inch diameter, and 22 inches long so that it could accommodate a 3-inch diameter x 6-inch long graphite cricible, which was fabricated from a graphite rod (Union Carbide, P2976).

The open end of the mullite tube was sealed vacuum tight with a copper sealing unit and a rubber O-ring. Below this sealing unit a copper water jacket was in contact with the outer diameter of the mullite tube to cool it and to prevent burning of the O-ring. Four electric fans were installed along the periphery of the furnace steel case to cool the top part of the mullite tube as well as to cool the aluminum braides, which connected the terminals of the heating elements. Gas inlet and outlet tubes were connected to the top of the copper sealing unit to control the gas atmosphere in the mullite tube. The alloys were generally formed in an argon gas atmosphere.

Alloy Preparation Procedure

Initially each metal component was weighed according to the desired composition of the alloy to be prepared. The maximum weight of the sample loaded into the crucible for each batch was about 600 grams. About 1/3 of the weighed aluminum was loaded into the

crucible, then the same portion of the weighed iron (and manganese when used) was placed on top of the aluminum. This loading sequence was repeated three times. The metal components used were large grains or chips, rather than fine powders, to facilitate the evacuation of remaining air in the mullite tube before heating.

The metal components were purchased from Alpha Products and had the following purities; aluminum 99.95%, iron 99.98%, and manganese 99.98%. After loading the metal samples into the crucible, it was placed on the bottom of the mullite tube with the aid of molybdenum wires, which were attached to the top of the crucible. The copper sealing unit and cooling jacket were assembled, followed by evacuation of remaining air in the tube with a vacuum pump. Then an oxygen-free grade argon gas (maximum oxygen content 0.5 ppm, Linde) was introduced into the tube after evacuation. This procedure was repeated three times to ensure complete evacuation of air in the tube to avoid any oxidation of metal samples during heating. Each evacuation and argon gas flow lasted for 10 minutes. Finally the argon gas was introduced into the tube at a flowrate of 40 liters/hour.

The furnace was heated to the desired temperature, 1523 K (1250^{o}C), about 100 K higher than the melting points of both types of alloys (Al/Fe = 50/50 wt %, Al-Fe-Mn = 59/38/3 wt %), for 24 hours. Near the end of the heating period, the alloy samples were heated to 1623 K (1350^{o}C) for 1 hour to avoid solidification of the molten alloy during casting of the alloy into a graphite mold.

After the heating the copper sealing unit was disassembled and the crucible was removed from the mullite tube. The molten alloy

was cast into graphite molds (1 inch I.D., 5 inch depth) and was air cooled. This casting step had to be done as quickly as possible before the molten alloy solidified. The casting process took about 2 to 3 minutes. Some degree of mixing of the alloy expected during this casting generated more homogeneous alloy samples. No further homogenization was attempted. After the solid alloy was cooled to room temperature, it was crushed with a pestle and a mortar to get the desired particle size (-25+50 mesh, U.S. sieve).

Alloy Characterization

X-ray diffraction. The x-ray powder diffraction technique has been used to identify phases present in the alloy samples with a Phillips Norelco vertical goniometer (Model XRG-2500). The alloy was crushed into a fine powder (passed through a 270 mesh U.S. series sieve) prior to analysis.

A collimated copper radiation (Cu K_α) was diffracted from the mounted sample to a graphite monochromator set and the radiation was transmitted to a scintillation counter. The tube current and the voltage were 20 mA and 35 kV, respectively. The sample was scanned between 10° and 85° (2θ) at a scanning speed of 2°/min.

Optical micrograph. An optical microscope (Olympus, Model BHM) was used to observe the surface of the etched aluminum alloy samples. A standard metallographic technique was used to prepare specimens for the optical micrograph.

The aluminum alloys (Al-Fe, Al-Fe-Mn) were mounted on a resin (Transoptic powder from Buhler). This mounted specimen was ground

and polished to expose an undistorted surface according to the procedures outlined in the literature.[153] The grinding/polishing was done with silicon carbide abrasive papers in order of decreasing particle size (240, 320, 400, and 600 grit size). The specimen surface was polished with magnesium oxide fine powders (Magomet from Buhler) on a rotating wheel as suggested by Mondolfo.[154] This final polishing step was continued until there was no evidence of scratch marks on the specimen surface. The absence of scratches was confirmed with the optical microscope.

The polished surface of the specimen was etched with an aqueous solution of sulfuric acid (20 volume percent at 343 K) for 30 seconds[155] to reveal the grain boundaries. Then the optical microscope was used to take pictures (Olympus camera, Model PM-10-M) of the specimen surface.

Electron microprobe analysis. The electron microprobe analysis has been carried out with an electron probe microanalyzer (Applied Research Laboratory, Model ARL-EMX) to identify metal phases in the alloys by elemental composition analysis. Although the x-ray diffraction technique can identify major phases in the sample, minor phases, if present, cannot be detected with the technique. Another objective was to obtain a positive confirmation of the presence of a ζ-$FeAl_2$ phase in the Al-Fe alloy (50/50 wt %). The Al-Fe alloy is expected to consist of two phases, ζ-$FeAl_2$ and η-Fe_2Al_5 phases, at equilibrium, but an x-ray diffraction pattern of the ζ-$FeAl_2$ phase is not available from the JCPDS file.

The specimens of the alloy samples used for electron microprobe analysis were prepared in the same manner as those used for the

optical micrograph. After fine polishing of the specimen, a thin film of carbon was deposited under vacuum on the surface of the sample to get better conduction of electrons, which prevents overheating or hot spot formation on the sample.

The electron probe microanalyzer had a fixed take-off angle (52.5^{o}) and was used at the following conditions:

Accelerating potential: 15 Kev

Emission current: 0.200 micro-ampere

Sample current: 0.04 micro-ampere

Count time: 40,000 integrated counts via a current to frequency converter.

The pure elements Al, Fe, and Mn were used to calibrate the noise by continuum x-rays for each determination of Al, Fe, and Mn content in the sample, respectively. ADP and LiF crystals were used to obtain $K_{\alpha 1}$ lines of aluminum and $K_{\alpha 1}$ lines of iron and manganese, respectively. A computer program (Magic V, developed by Tracor-Northern, Inc.) was used to process the raw data. The computer program has a built-in subprogram, which makes the ZAF correction.

Alloy Activation

Activation Reactor

The Raney catalysts were activated in a four-necked 1-liter resin flask. The reactor (Figure 11) was immersed in a constant temperature water-bath (number 1 in Figure 11) whose temperature was controlled by a temperature controller (Haake, Model E-2) (3) which also circulated water in the bath.

Figure 11

Alloy Activation Reactor

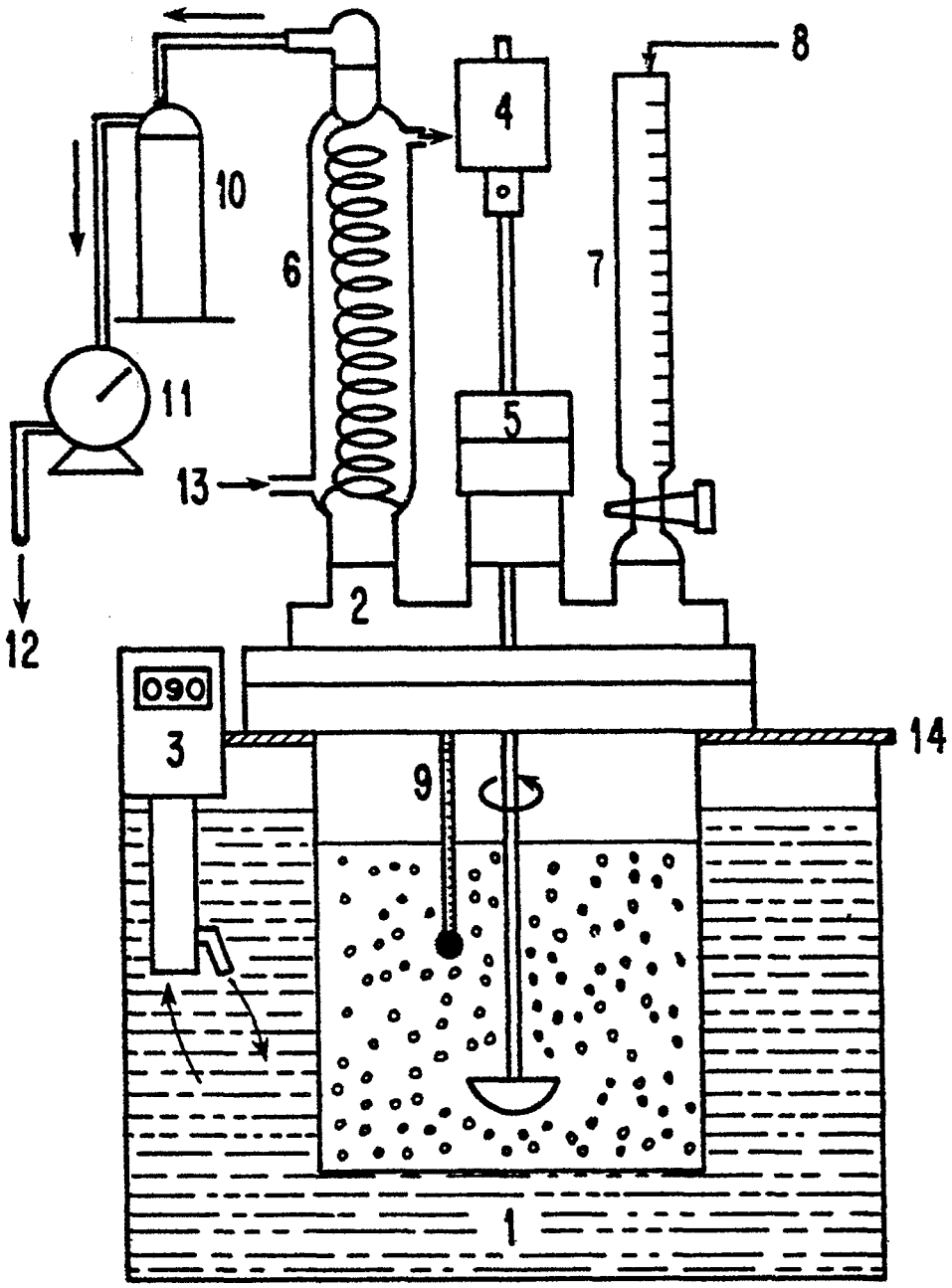

1 · Water bath
2 · Four-necked flask
3 · Bath temp. controller
4 · Stirring moter
5 · Teflon seal
6 · Condenser
7 · Burette
8 · Caustic solution
9 · Thermometer
10 · Safety bottle
11 · Dry testmeter
12 · Hydrogen exit gas
13 · Cooling water
14 · Reactor support

The aluminum component in the alloy was leached by a sodium hydroxide solution. The temperature of the solution in the reactor was monitored by a thermometer or a thermocouple in the reactor. The temperature of the bath was adjusted to give a constant reactor temperature during the leaching process. A water-cooled condenser (6) was connected to the top of the reactor to condense any escaping water vapor from the solution, especially at a high leaching temperature. A burette (7) was attached to the reactor only when sodium hydroxide solution was added during the leaching process and a glass stopper was used when alloy particles were added into the reactor during the leaching period. The volume of hydrogen gas produced during the leaching was measured by a dry testmeter (11) and was a convenient means for estimating the extent of leaching.

The activated alloy particles (Raney catalyst) were transferred to the wash apparatus (Figure 12) at the end of the leaching process where the remaining caustic solution was removed. A deionized water reservoir (number 4 in Figure 12) supplies fresh water continuously to the wash flask (1). The flask was equipped with gas inlet and outlet connections to provide an inert gas atmosphere in the flask during the washing process. Continuous washing was achieved with a spent wash water overflow. The water in the flask was constantly stirred during the washing process.

Activation Procedure

The alloys prepared in this investigation were activated by two methods: caustic addition method and alloy addition. The primary difference between the two procedures is the reactant added to

Figure 12

Activated Raney Catalyst Washing Apparatus

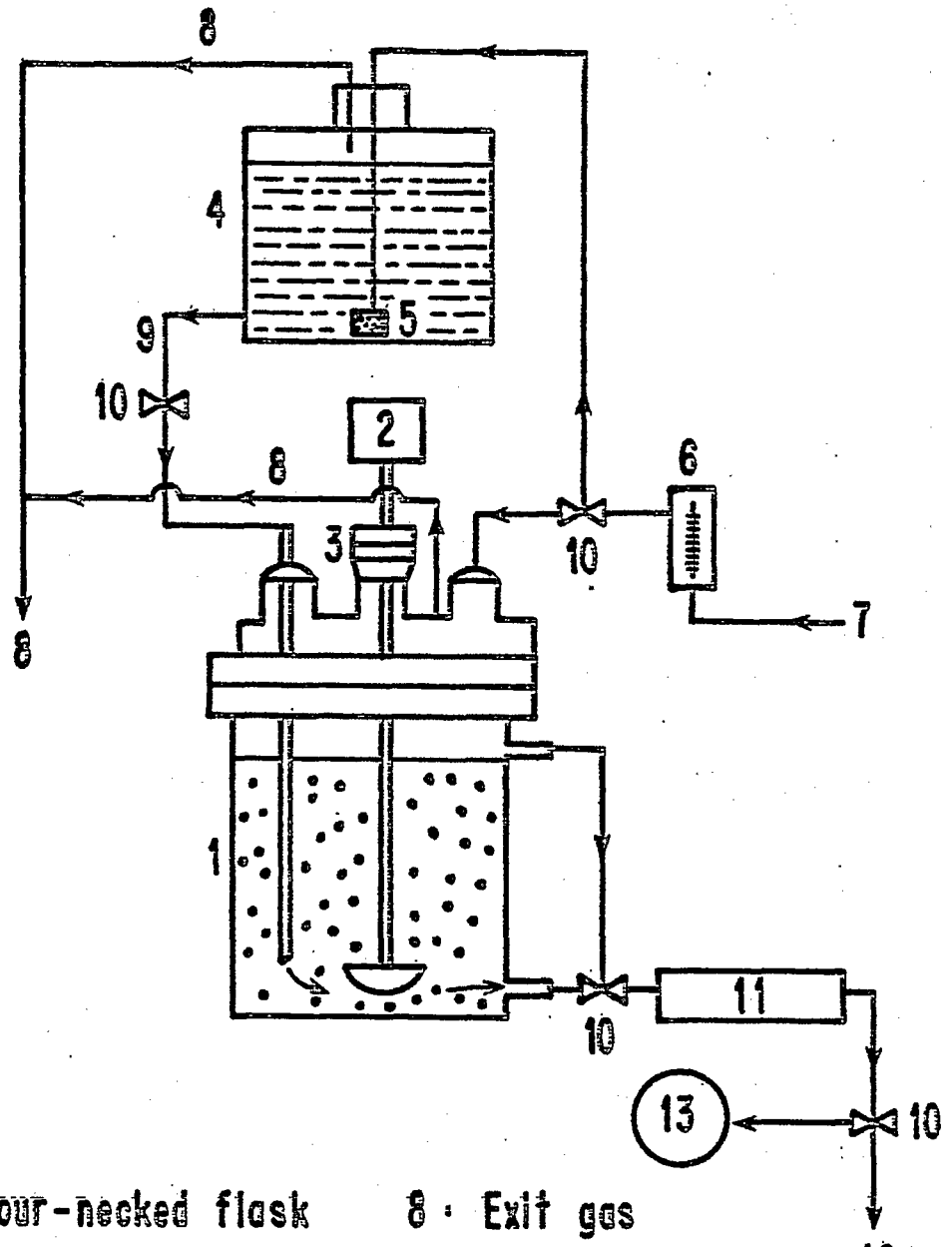

1 : Four-necked flask
2 : Stirring motor
3 : Teflon seal
4 : Water reservoir
5 : Air stone
6 : Rotameter
7 : Argon gas
8 : Exit gas
9 : Washing water
10 : Stopcock
11 : Catalyst trap
12 : Water drain
13 : pH meter

reactor during the leaching process. The sodium hydroxide solution is added to the reactor in the caustic addition method whereas the alloy particles are added to the reactor in the alloy addition method.

Caustic addition method. The deionized water reservoir was degassed for about 3 hours with flowing argon before starting the activation of the alloys. This argon flow was quite efficient in removing gases dissolved in the water, especially, oxygen. The oxygen was removed to below 1 ppm. The desired amount of alloy and deionized water were added into the activation flask and were constantly stirred. The temperature of the reactor was increased to a temperature 10 to 20 K lower than the actual leaching temperature. The final leaching temperature depends on the amount of alloy used and the desired leaching temperature. The alloy-water slurry was equilibrated at the water-bath temperature.

If 50 grams of an alloy was to be activated, 250 cm^3 of deionized water was added into the flask at the outset. Then 250 cm^3 of a 40 wt % sodium hydroxide solution was added as follows: 5 cm^3 of the sodium hydroxide solution was added at 3-minute intervals for 90 minutes. The remaining 100 cm^3 was added in 50 cm^3 increments at 10-minute intervals. The total elapsed time for the addition process was about 2 hours. At the end of 2 hours most of the aluminum was leached out, as indicated by the volume of hydrogen gas evolved during the leaching process. The alloy particles were subjected to an additional 90 minutes leaching until there was no evolution of hydrogen gas. The temperature of the reactor was kept constant by adjusting the time interval between successive caustic additions or by using a

stainless steel cooling tube, which was immersed in the reactor and through which cold water was passed. The temperature fluctuations in the reactor were less than $\pm$ 5 K from the desired leaching temperature during the course of an experiment.

After the leaching process was completed, the sodium hydroxide solution was decanted and the activated alloy was washed with deionized water 5 times. Then the alloy particles were transferred into the washing flask where any remaining caustic was removed. The activated alloy was washed until the decanted liquid indicated the same pH value as that of the fresh deionized water (ph $\approx$ 7). The pH value was monitored by a Corning pH meter (Model 12). The activated alloy was washed with 95% ethanol 3 times, followed by washing with absolute ethanol 3 times. The activated alloy, that is, the Raney catalyst, was then stored under absolute ethanol and was kept at 273 K in a refrigerator. In the caustic addition method the alloy was exposed initially to a very low concentration of sodium hydroxide solution (low pH value), followed by exposure to an increasingly high concentration (high pH value) as the sodium hydroxide solution was added to the reactor.

Alloy addition method. In the alloy addition method the alloy particles were divided into 10 equal amounts and each portion of the alloy was added to the reactor, which contained 500 cm^3 of 20 wt % sodium hydroxide solution, at 3-minute intervals. If 50 grams of an alloy was to be activated, 5-gram samples of the alloy were added to the reactor at 3-minute intervals for 30 minutes. Additional leaching was done for 90 minutes. The procedure for washing the catalyst was the same as described for the caustic addition method.

In the alloy addition method the alloy was exposed to a high concentration of sodium hydroxide from the beginning. A more vigorous evolution of hydrogen gas was observed, even in the early stage of the activation, when compared to the caustic addition case.

Preparation of Precipitated Catalysts

A precipitated iron and a coprecipitated iron-manganese catalyst were also prepared following the procedures of Yang[4] and Tillmetz.[2] An appropriate amount of iron nitrate (about 500 grams), $Fe(NO_3)_3 \cdot 9H_2O$, was dissolved in 1 liter of hot distilled water. Manganese nitrate solution [50 %, $Mn(NO_3)_2$] was added to the aqueous solution of iron nitrate when a coprecipitated Fe-Mn catalyst was prepared. The amount of manganese nitrate was adjusted to give a desired composition of the catalyst, that is, the desired Fe/Mn atomic ratio. The solution was continuously stirred and heated to the boiling point.

The precipitated catalyst was formed by slowly adding an ammonium hydroxide solution (20% as NH_3) to the metal nitrate solution. Near the end of the addition of ammonium hydroxide the pH value of the solution was monitored and the pH value was kept higher than 9 to ensure complete precipitation of the metal ions. After the precipitation the wet catalyst cake was filtered and washed with boiling distilled water until there was no trace of nitrate ion in the filtrate. The presence of trace nitrate ion was checked by the brown ring test, suggested by Sorum and Legowski[156] as follows: In a test tube 2 or 3 drops of filtrate is mixed with 10 drops of concentrated sulfuric acid and is cooled for a few minutes. Then 3

drops of iron sulfate solution (0.2 M, $FeSO_4$) is added in the tube. The presence of trace nitrate ion is confirmed by formation of a brown ring on the top layer of the solution in the test tube.

The wet catalyst cake was dried in air in an oven at 393 K for 24 hours and was crushed to the desired particle size (-25+50 mesh). All the chemicals used in the preparation of these catalysts were reagent grade from J. T. Baker.

Catalyst Characterization

X-Ray Diffraction

Phase identification. The identification of phases in the Raney catalysts was accomplished by x-ray powder diffraction. The Phillips Norelco vertical goniometer, which was used to analyze the alloy samples, was also used to analyze the Raney catalysts.

The sample preparation and the operational procedures were discussed previously. The only difference in the preparation of the Raney catalyst samples was the coating of the fine catalyst powders with Collodion solution (2% nitrocellulose solution in amylacetate from Bühler) to prevent oxidation of samples during the test. The catalysts were ground to a fine powder under absolute ethanol. After decanting the excess ethanol, the catalyst was coated with the Collodion solution by mixing the catalyst with a few drops of Collodion. The catalyst slurry was mounted on an x-ray diffraction sample holder and dried in air before the x-ray analysis was performed.

Crystallite size measurement. The crystallite size of the α-Fe in the Raney catalyst was determined by an x-ray line broadening technique. The sample preparation procedures were the same as those for the phase identification study. The operating procedures were the same as those described previously, however, the sample was scanned at a scanning speed of $1/2^{o}$/min (2θ) during the crystallite size measurements.

Alpha-quartz powder (5 micron size from Minusil) was used as a reference standard. The instrumental broadening was determined at half-maximum intensity from a diffraction peak of the alpha-quartz at (2, 0, 1) plane ($2\theta = 45.78^{o}$).

BET Surface Area

The total surface areas of the Raney catalysts were measured at liquid nitrogen temperature with a Micromeritics Surface and Pore Volume Analyzer (Model 2100). Before mounting the catalyst sample on the BET analyzer, most of the ethanol was evacuated at room temperature by a rotary vacuum pump. Degassing was done at 393 K for 24 hours under high vacuum ($< 1.37 \times 10^{-2}$ Pa). The operating procedure for surface area measurements is thoroughly discussed and outlined in the Instruction Manual for the model 2100.[157]

Atomic Absorption

The composition of the Raney catalysts have been determined by atomic absorption spectroscopy (Instrumental Laboratory, Model IL-351).

Sample preparation. Initially, the wet catalyst, stored under absolute ethanol, was dried in the sample holder (Figure 13) by heating the sample to 353 K under vacuum by a rotary vacuum pump. Usually an hour was required before the catalyst weight stabilized. Deionized water was introduced into the sample from the top of the sample holder to immerse the catalyst in water. The catalyst-water slurry was transferred to a 100 cm^3 flask where the catalyst was completely dissolved in 50 cm^3 of concentrated hydrochloric acid. After the catalyst had been completely dissolved, the solution was diluted with deionized water to a volume of 100 cm^3. The concentration of the solution was then adjusted to about 10,000 ppm total metal content.

The solution of dissolved catalyst was diluted to a concentration range with respect to each element in which the concentration and the absorbance exhibited a linear relationship. The dilution was carried out just prior to the analysis for each element, since some of the elements, such as iron, undergo precipitation at a very low concentration leading to erroneous results.

Operation. The atomic absorption spectrometer was warmed up for at least half an hour before each analysis. The Al, Fe, and Mn hollow cathode lamps were used for the elemental analysis of Al, Fe, and Mn, respectively. The instrument was set for the standard operating conditions for each element before igniting the flame. These conditions included the lamp current, the wavelength of radiation beam, the silt width, and the air fuel ratio.[158] The instrument was readjusted by adjusting the above-mentioned parameters

Figure 13

Raney Catalyst Sample Holder

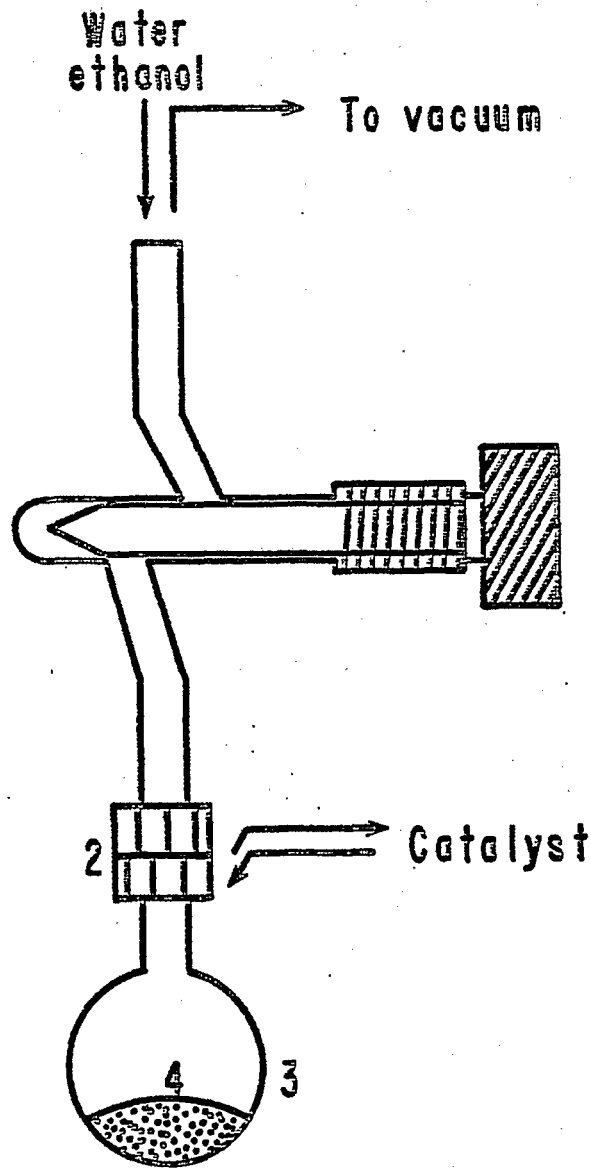

1. Vacuum stopcock
2. Vacuum tight O-ring joint
3. Sample holding flask
4. Catalyst

after igniting the flame to give a maximum sensitivity as specified in the manual.

Several standard solution samples containing different concentrations of a specific element were aspirated into the burner head at a flowrate of 5 cm^3/min after the adjustment of the instrument. The absorbance values of the standard samples were obtained and an absorbance-concentration calibration curve was obtained. This procedure was repeated at least twice for each analysis. The absorbance value of an unknown sample was obtained and the corresponding concentration was determined from the calibration curve.

Thermogravimetric Reduction Study

A thermogravimetric reduction study was conducted to determine an optimum reduction condition (reduction temperature and reduction time) for precipitated and Raney iron and iron-manganese catalysts. A DuPont TGA Model 951 was used for the thermal analysis of the precipitated catalysts. A Perkin-Elmer Model TGS-2 was used for the thermal analysis of the Raney catalysts, since there was an electromagnetic interaction between the DuPont TGA furnace and the Raney catalysts.

A schematic of the thermogravimetric system is presented in Figure 14. The hydrogen (Linde, 99.999% purity) and helium (Linde, 99.995% purity) gases were purified by a hydrogen purifier (Matheson, Model 8362) and a Hydroxpurifier (Matheson, Model 8301), respectively.

A cold trap (mixture of ice and acetone) was used between the hydrogen purifier and a vacuum pump to prevent any intrusion of vacuum

Figure 14

Schematic of the Thermal Analysis

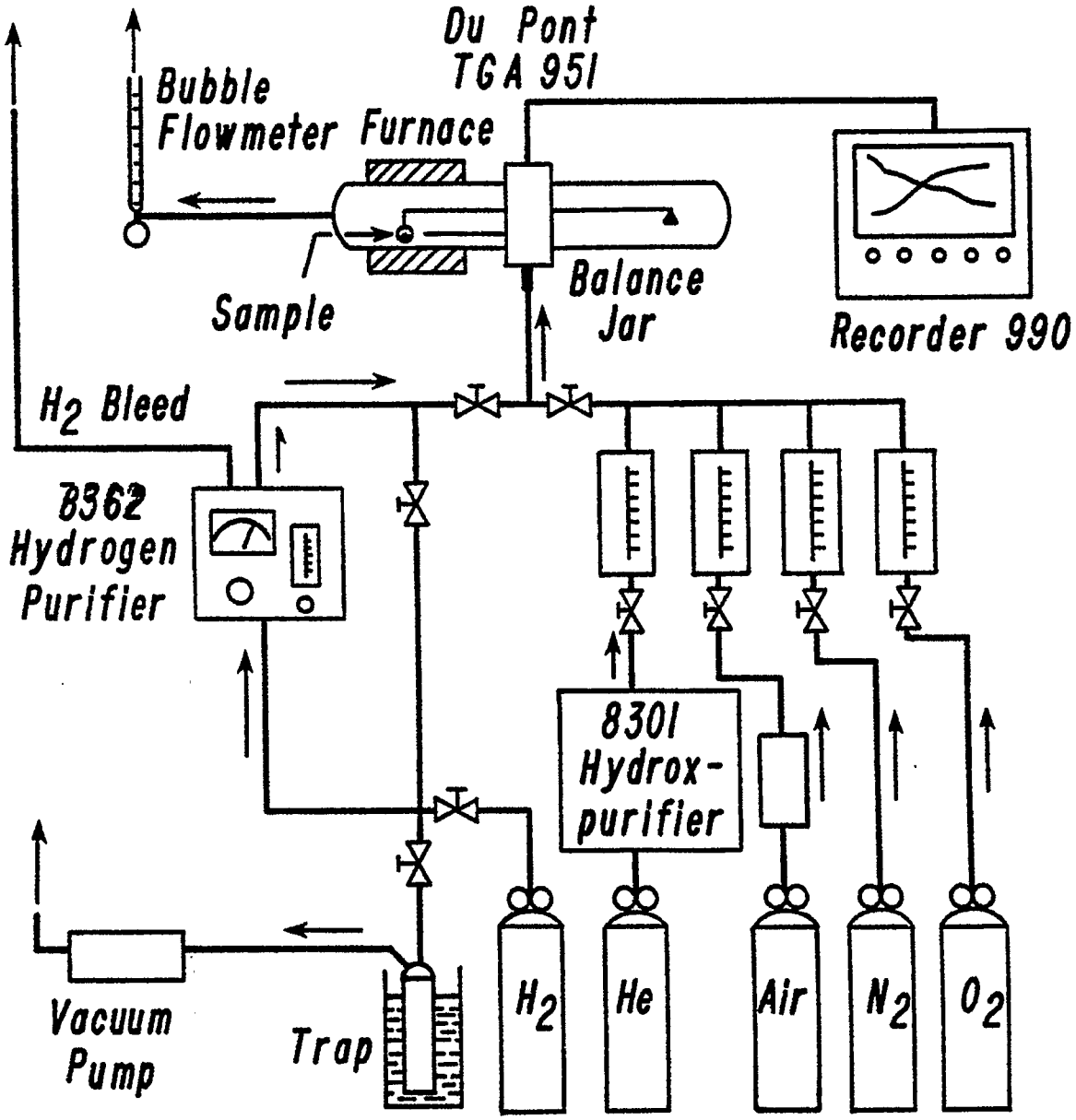
Du Pont
TGA 951
Bubble
Flowmeter
Furnace
Sample
Balance
Jar
Recorder 990
H2 Bleed
8362
Hydrogen
Purifier
8301
Hydrox-
purifier
Vacuum
Pump
Trap
H2
He
Air
N2
O2

pump oil vapor into the purifier. Air (Matheson, ultra-zero grade) was purified by passage through a molecular sieve column and was used without further purification. The flowrate of each gas was controlled by a rotameter (Fisher-Porter, Model 10A1376) to give 50 cm^3/min. The flowrates were measured by a bubble flowmeter. Typically 20 to 40 mg of the catalyst was loaded onto a sample pan which was then placed in the furnace. The instrument was operated in both the temperature programmed and isothermal modes and the weight loss was recorded on a chart recorder.

Catalyst Screening Test

Fixed-Bed Reactor Apparatus

A high pressure fixed-bed reactor was built to test the activity and selectivity of the catalysts. A schematic of the fixed-bed unit is presented in Figure 15.

A mixture of carbon monoxide and hydrogen (Linde, primary standard) passed through a column of activated carbon to remove any impurities, such as water and metal carbonyls. The activated carbon was regenerated in flowing helium at 423 K for 4 hours. The flowrate of the reactant gas into the reactor was controlled by a mass flow controller (Union Carbide, Model FM 4550). Hydrogen gas (Linde, 99.99% purity), purified by a Deoxo unit (Matheson, Model 64-1010), was used for the in-situ reduction of the catalysts. Helium gas (Linde, 99.995% purity) was used without further purification to leak test the apparatus after the reactor was placed on the unit.

The fixed-bed reactor consisted of a 1-inch O.D. and 1/2-inch I.D. stainless steel tube, which was embedded in a 3/4-inch thick

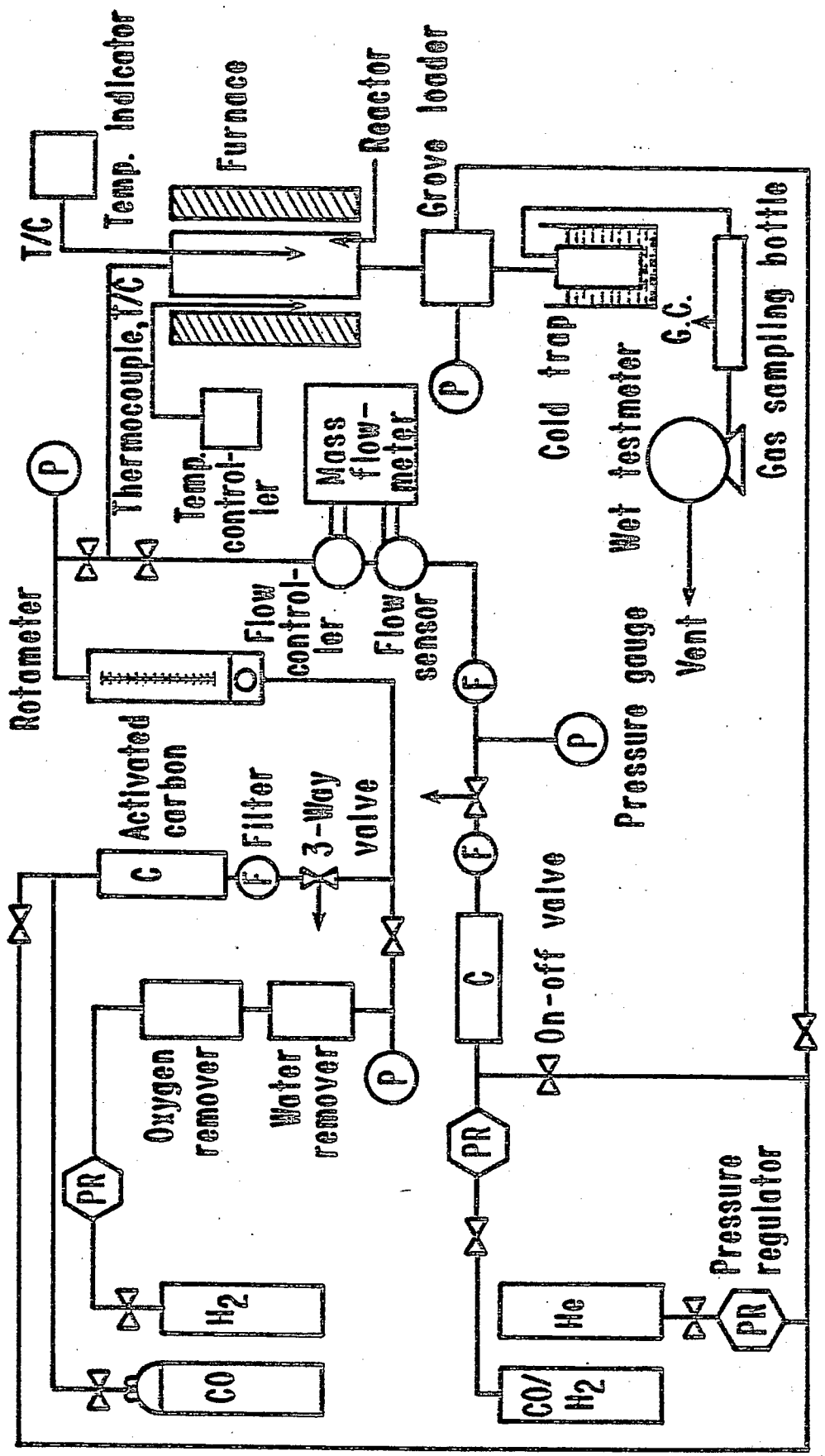
T/C
Temp. Indicator
Furnace
Reactor
Grove loader
Thermocouple, T/C
Temp. control-ler
Mass flow-meter
Cold trap
Wet testmeter
G.C.
Gas sampling bottle
Rotameter
Flow control-ler
Flow sensor
Activated carbon
Filter
3-Way valve
Pressure gauge
Vent
Oxygen remover
Water remover
On-off valve
Pressure regulator
H2
CO
He
CO/H2
PR
P
F
C

cylindrical copper block to achieve a uniform temperature profile along the reactor length. An electric heating furnace was used to heat the reactor. The furnace was controlled by a temperature controller (Love, Model 49). The temperature profile of the catalyst bed was monitored by a travelling thermocouple in a thermowell on the centerline of the reactor.

The catalyst bed was positioned in the middle of the reactor. Ceramic packing (Denstone, -25+50 mesh, Norton Co.) was placed in the zone above the catalyst as a preheater. The ends of the reactor tube were sealed by stainless steel gaskets. Detailed design drawings of the reactor are included in Appendix B.

A Grove back-pressure regulator was installed after the reactor to maintain the reactor pressure during the reaction by releasing excess pressure to atmospheric pressure. The exit gas passed through a cold trap, in which high boiling products were trapped. The volume of the exit gas was measured by a wet test-meter. A gas sampling bottle was used to take gas samples for gas chromatography.

Procedures of Fixed-Bed Run

The first step in the fixed-bed run was to load a weighed amount of catalyst into the reactor. Since the Raney catalyst is quite pyrophoric when exposed to air, a special handling procedure was required to load it into the reactor. Raney catalysts are usually weighed with a picnometer when the density of the catalyst is known. Thus the density of each different catalyst must be known or measured in order to measure the weights of different catalysts. An

alternative loading procedure has been devised for this investigation: An appropriate amount of catalyst was transferred from the storage bottle into a sample holder (Figure 13). The excess ethanol was decanted and the remaining ethanol was evacuated at 353 K by a rotary vacuum pump. After about an hour the weight change was quite negligible. The catalyst weight was obtained by difference between the weight of an empty sample holder and that of a loaded one. The catalyst was immersed again in absolute ethanol by adding ethanol to the sample holder through the inlet. The catalyst-ethanol slurry was then immersed in deionized water, since pure ethanol was dried up quickly within a few minutes from the catalyst surface and the catalyst was exposed to air during loading the catalyst into the reactor. Loading the catalyst into the reactor and leak testing of the fixed-bed unit took about 15 minutes.

After confirming that there were no leaks in the system by pressurizing the system with helium at the reaction pressure, the wet catalyst was dried by flowing hydrogen gas through the catalyst bed for about an hour at room temperature and then at 353 K for another hour. The catalyst was heated slowly to the desired reduction temperature (648 K for the Raney catalysts and 673 K for the precipitated catalysts) under flowing hydrogen at a pressure of 150 KPa and a space velocity of 3 cm^3 (STP)$g^{-1}s^{-1}$. It took about 2 hours. The reduction was continued for 5 hours at the reduction temperature.

After reduction the reactor was cooled in flowing hydrogen to the reaction temperature, usually 423 K. When the reactor temperature reached 423 K, the hydrogen flow was replaced with a

mixture of carbon monoxide and hydrogen. The reactor pressure was increased slowly to the reaction pressure, 1465 KPa (200 psig). The following standard conditions were used for screening all the catalysts: a total reaction pressure of 1465 KPa (200 psig), a reactant space velocity of 3.0 $cm^3g^{-1}s^{-1}$, a hydrogen-to-carbon monoxide ratio of 2, and a reactor temperature range of 423 - 473 K. The flowrate of the reactant gas mixture was adjusted to give a desired space velocity as follows: First the desired flowrate was estimated by multiplying the catalyst weight measured to a space velocity desired. Then the flowrate was controlled by adjusting the flowmeter setting to the desired flowrate, which was read from a flowrate-flowmeter setting calibration chart.

The reactant gas was allowed to flow through the reactor until the catalyst activity and selectivity reached a steady state at a reaction condition. This was checked by intermittent product gas sampling and analysis by a gas chromatograph from the start of the fixed-bed run. If two successive gas chromatographic analyses of the exit gas were the same, it was assumed that the catalyst had reached a steady state at the reaction condition. It took about 4 to 5 hours at 423 K to reach steady state, depending on the catalyst type. The activity of the catalyst was evaluated in the temperature range of 423 - 473 K by increasing the reactor temperature in 10 K increments. The flowrate of the exit gas was measured for each evaluation at the different temperatures to provide a carbon mass balance.

Product Analysis

The product from the hydrogenation of carbon monoxide was analyzed by a gas chromatograph (Hewlett Packard, Model 5830A), using both TCD and FID detectors. The TCD detector was used for carbon monoxide and carbon dioxide gases, and the FID was used for all hydrocarbon products up to C_7. Dual columns of Chromosorb 102 (80 - 100 mesh, 20 ft) were used for the gas analysis. Since most of the activity tests were conducted at low levels of carbon monoxide conversion, there was essentially a negligible amount of liquid products (water, alcohol, and high molecular weight hydrocarbons) collected in the cold trap in all runs. Thus it was not possible to collect sufficient liquid hydrocarbon sample to perform product analysis under the test conditions.

The compositions of the product gas were analyzed as follows: The absolute response areas for pure methane and carbon monoxide were obtained by injecting 1 cm^3 of pure methane and carbon monoxide just prior to each activity test for a given catalyst. These absolute response areas may change depending on the conditions of detectors and had to be determined at least on a daily basis. The absolute response areas from 1 cm^3 injections of other pure components were calculated by a computer program, instead of injecting the pure samples into the gas chromatograph, based on the relative response factor values listed in the program and the absolute response areas obtained from 1 cm^3 injections of pure methane and carbon monoxide (see Appendix D for an example of the calculation). One cm^3 of the product gas was taken by a syringe from a gas sampling bottle and was injected into the gas chromatograph for composition analysis of

the product gas. All the pertinent data, such as response area for each component in the product, input reactant and output product gas flowrates, and reaction conditions, were fed into the program to estimate the catalyst activity and product selectivity (see Appendix C for an example).

The catalyst activity was defined in terms of carbon monoxide conversion, which was defined in two ways in the program as follows:

i) Carbon monoxide conversion % (output basis): D2

$$D2 = (1 - X_2/K) \times 100 \tag{63}$$

$$X_i = V_i N_i$$

$$K = \Sigma X_i = \Sigma V_i N_i \ .$$

V_i is the mole fraction of component i in the product gas, N_i is the number of carbon atoms in the molecular formula for component i (e.g., $N_i = 2$ for ethane or ethylene), X_2 is the mole fraction of carbon monoxide in the product, and K is the sum of carbon atom mole fraction of all the product containing carbon atoms. This conversion represents the actual carbon monoxide conversion within experimental limits of product analysis (including liquid and solid high molecular weight hydrocarbons).

ii) Carbon monoxide conversion % (input - output basis): D1

$$D1 = [1 - X_2 \cdot F_1/(C_1 \cdot F_1)] \times 100 \ . \tag{64}$$

In Equation (64), F_1 is the flowrate of input reactant gas, F_2 is the flowrate of exit product gas, and C_1 is the mole fraction of carbon monoxide in the reactant gas.

The two conversions should agree within an experimental error if all the products can be collected and counted at a steady state reaction condition. Under actual experimental conditions, the second definition was more likely to be in error than the first definition. The first definition seems to be reasonable under the test conditions in which the carbon monoxide conversion was low enough to ensure that negligible amount of high molecular weight hydrocarbons was formed. Therefore, the first definition was exclusively used when comparing activities of different catalysts.

The selectivity was also defined in two ways:

i) Product carbon atom selectivity: Y_i

$$Y_i = \frac{X_i}{K_1} \times 100 \qquad (65)$$

$$K_1 = K - X_2 .$$

In Equation (65), K_1 is the sum of carbon atom mole fraction of all the products containing carbon atoms except for carbon monoxide, that is, carbon dioxide plus all hydrocarbons.

ii) Hydrocarbon selectivity: Z_i

$$Z_i = \frac{X_i}{K_2} \times 100 \qquad (66)$$

$$K_2 = K - X_2 - X_3 .$$

In Equation (66), K_2 is the sum of carbon atom mole fraction of all the hydrocarbons excluding carbon monoxide and carbon dioxide from the product. The first definition includes carbon dioxide in the product, while the second one does not.

Carbon Mass Balance

A carbon mass balance was computed for each fixed-bed run. A carbon mass balance error, G, was defined as follows:

$$G = (G_1 - G_2)/G_1 \times 100 \tag{67}$$

$$G_1 = C_1 \times F_1 \times (650/760)/(82.05 \times 291.2)$$

$$G_2 = K \times F_2 \times (P_1/760)/[82.05 \times (273.2 + T_1)]$$

where P_1 is the ambient pressure in mm Hg and T_1 is the ambient temperature in degree centrigrade at the time of the activity test. G_1 is the total input number of moles of carbon atoms in the reactant gas per unit time and G_2 is the total output number of moles of carbon atoms in the product from the reactor per unit time. The input flowrate of the reactant gas was calibrated at a standard condition, that is, an ambient pressure of 650 mm Hg and an ambient temperature of 291.2 K ($18^{o}C$); however, the output flowrate of the product gas was measured at various ambient conditions. The above mass balance equation is meaningful under actual testing conditions only when the formation of high molecular weight hydrocarbon products is negligible. When there is a considerable amount of liquid and solid hydrocarbons formed, this must be taken into account for the

carbon mass balance. A sample calculation for the carbon mass balance is included in Appendix D.

RESULTS AND DISCUSSION

Alloy Characterization

X-Ray Diffraction

The x-ray diffraction technique was used to identify the metal phases present in the aluminum alloys. Only the single phase, θ-$FeAl_3$, was expected for an Al-Fe-Mn alloy (Al/Fe/Mn = 59/38/3 wt %) according to the ternary alloy phase diagram (Figure 5). Since the atomic size of manganese is similar to the size of iron, manganese atom can be easily incorporated into the crystal lattice of $FeAl_3$ phase by replacing the iron atom. The actual formula of the phase would be $(Fe,Mn)Al_3$.

The x-ray powder diffraction pattern of the Al-Fe-Mn alloy was identical to the diffraction pattern of $FeAl_3$ filed by JCPDS[140] based on a comparison of the 2θ values of the peaks and the relative intensities of the peaks (Table 2). Therefore, the major phase present in the Al-Fe-Mn alloy was the $FeAl_3$ phase, although some minor phases may be present and remained undetected by x-ray diffraction.

The x-ray diffraction pattern data for the Al-Fe alloy (50/50 wt %) is listed in Table 3. Two phases, ζ-$FeAl_2$ and η-Fe_2Al_5, were expected according to the binary alloy phase diagram (Figure 4). The Al-Fe alloy had the diffraction peaks of Fe_2Al_5 phase in

Table 2

X-Ray Diffraction Data for Al-Fe-Mn Alloy

Miller Index (hkl)[a]	2θ (Degree)	Relative Intensity $FeAl_3$[b]	Relative Intensity Al-Fe-Mn Alloy
(10,2,0)	21.93	40	13
(12,2,0)	22.49	40	13
(4,4,0)	24.16	60	13
(2,2,2)	25.13	60	17
(8,0,2)	26.75	20	11
(6,2,2)	26.51	20	6
(3,3,3)	27.33	10	11
(5,3,3)	38.44	60	8
(11,1,3)	40.04	40	9
---	40.39	40 β	--
(18,2,2)	42.61	40	19
(6,6,2)	43.25	100	57
(571,2220)	43.47	40	32
(14,6,0)	43.91	40	40
(16,4,2)	44.36	100	100
(0,0,4)	44.82	100	51
(553,2 3 11)	45.79	20	11
(0,8,0)	47.04	40	13
(480,1533)	47.57	20	6
(22 2 4,30 2 2)	64.17	60	26
(14,6,4)	65.18	60	19
(24,0,4)	66.22	20	6
(0,8,4)	66.76	40	9
(11,9,3)	68.42	20	--
(0,0,6)	69.50	40	--
(0,12,0)	73.32	60	9

[a] Miller Index for $FeAl_3$ phase.

[b] Diffraction pattern of $FeAl_3$ phase from JCPDS file.[140]

Table 3

X-Ray Diffraction Data for Al-Fe Alloy

Miller Index (hkl)[a]	2θ (Degree)	Relative Intensity Fe_2Al_5[b]	Relative Intensity Al-Fe Alloy
	19.0		40
	21.0		15
	22.2		5
(2,0,0)	23.0	25	15
	24.4		25
	24.8		24
	25.2		17
	26.8		15
(020,111)	27.9	40	20
	35.5		7
	37.2		5
	38.8		13
	42.7	100	80
(0,0,2)	42.8	100	85
	43.7		100
(1,3,0)	44.1	100	86
	44.5		40
	44.8		45
(1,1,2)	46.8	10	3
	47.6		5
(202,131)	49.5	4	6
	50.0		14
	61.7		8
	63.6		13
	64.2		12

[a]Miller Index for Fe_2Al_5 phase.

[b]Diffraction pattern of Fe_2Al_5 from JCPDS file.[140]

addition to a set of unidentified peaks, which is supposedly the diffraction peaks of the $FeAl_2$ phase. The diffraction pattern of the Al-Fe alloy is illustrated in Figure 16. The dotted lines are the diffraction peaks of the Fe_2Al_5 phase. From the x-ray diffraction study of the Al-Fe alloy, only the Fe_2Al_5 phase could be identified due to the unavailability of information on the diffraction pattern of $FeAl_2$ phase. Other characterization techniques should be used to confirm the presence of the $FeAl_2$ phase.

Optical Micrograph

The Al-Fe (50/50 wt %) alloy has been examined with an optical microscope. The alloy sample was heat treated at 1173 K for 2 days in an evacuated quartz tube.

The optical micrographs of the Al-Fe alloy at two different magnifications, 100 and 400, are presented in Figure 17. The micrographs revealed the existence of two regions with different shades indicating the presence of two phases in the alloy. The lightly shaded phase was embedded in the second, darkly shaded phase. A grain size of about 100 microns and dendrite structures were observed. (The elongated-blade-shaped grains joined like tree branches shown on the upper left corner of the picture with a higher magnification in Figure 17.)

Electron Probe Microanalysis

Electron probe microanalyzer has been used to identify phases present in the Al-Fe (50/50 wt %) and Al-Fe-Mn (59/38/3 wt %) alloy and to check the homogeneity of samples. An unetched sample of the Al-Fe alloy, heat treated at 1173 K for 2 days, was scanned

Figure 16

X-Ray Diffraction Pattern for an
Al-Fe Alloy

Composition: Al/Fe = 50/50 wt %

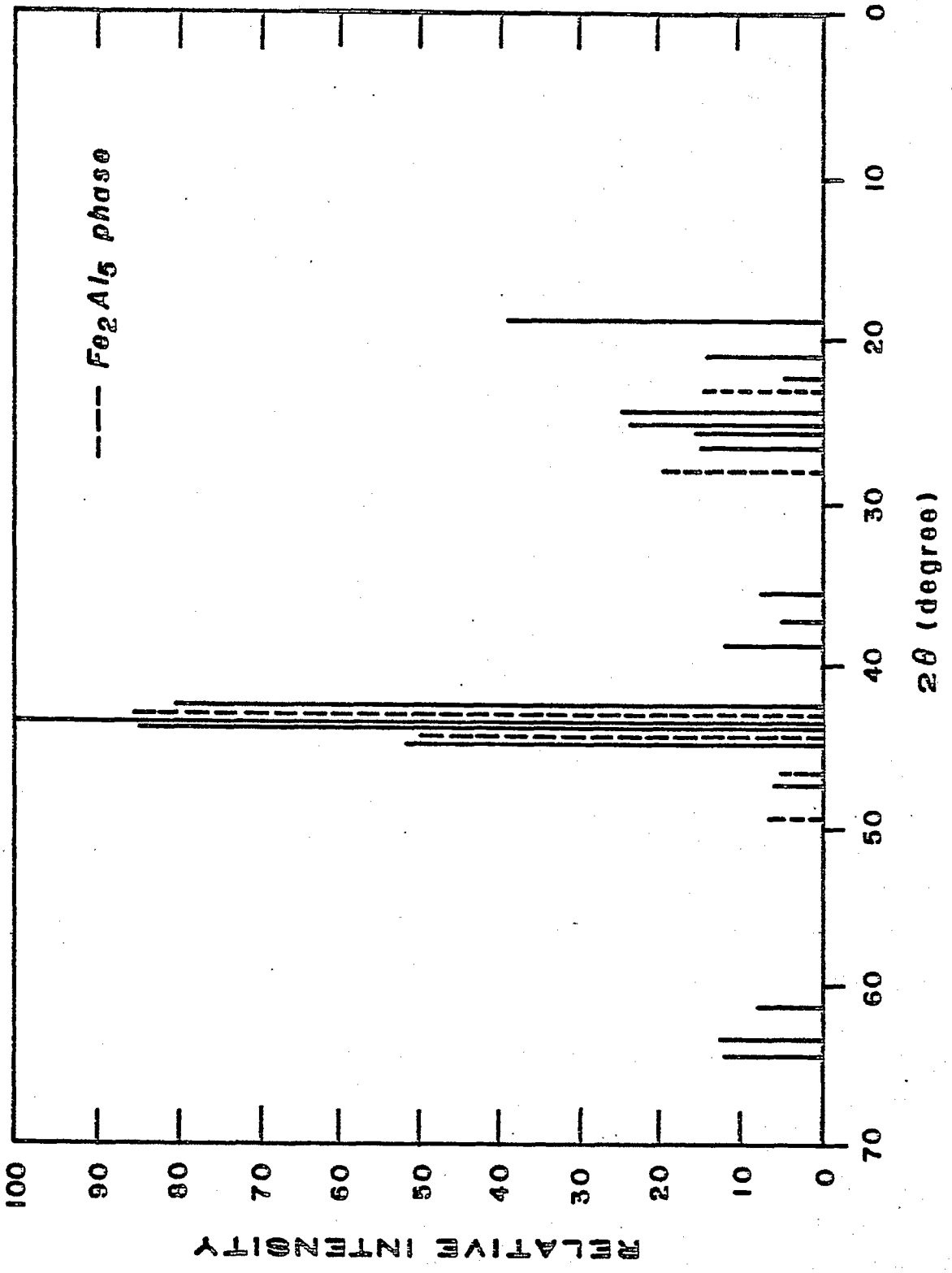
--- Fe_2Al_5 phase
RELATIVE INTENSITY
100
90
80
70
60
50
40
30
20
10
0
0
10
20
30
40
50
60
70
2θ (degree)

Figure 17

Optical Micrograph of Al-Fe Alloy

Composition: Al/Fe = 50/50 wt %

Heat Treatment: 1173 K, 48 hours

Etching: 20 volume percent sulfuric acid solution at 343 K for 30 seconds

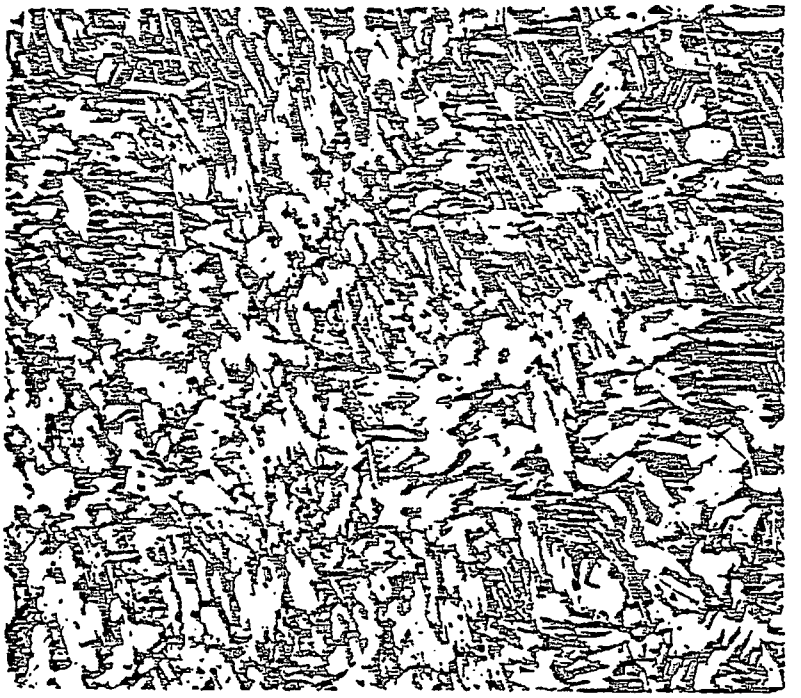

100 x ⌊——⌋ 100 μ

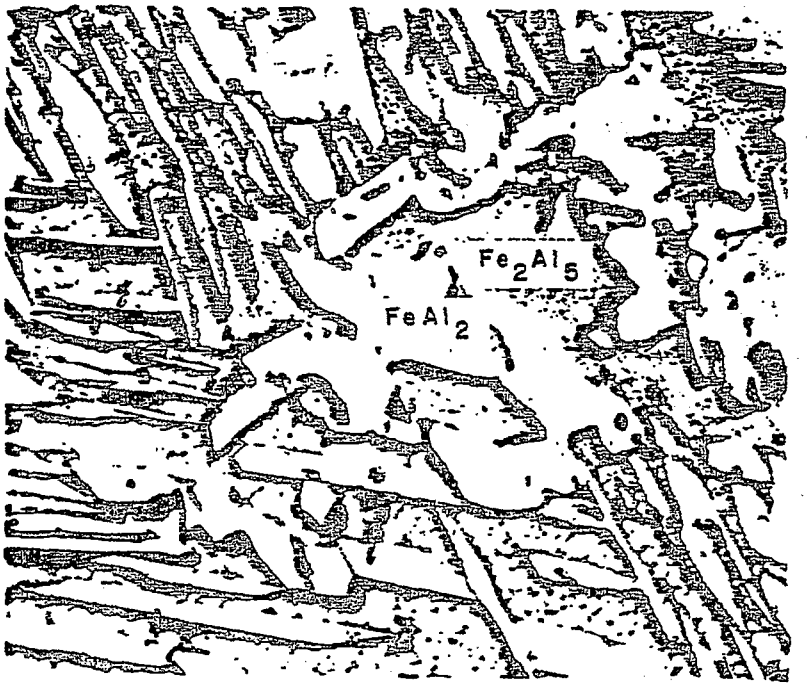

400 x ⌊——⌋ 50 μ

with the microprobe analyzing 100 points along the surface of the alloy with each point 10 microns apart. Apparently, there were two regions with different metal compositions. One region had a composition of 55.2 wt % of aluminum and 44.8 wt % of iron, which corresponded to a formula of Fe_2Al_5. The other region had a composition of 49.5 wt % of aluminum and 50.5 wt % of iron, which corresponded to the formula $FeAl_2$. From this microprobe data it has been confirmed that the Al-Fe alloy consisted of two phases, ζ-$FeAl_2$ and η-Fe_2Al_5.

Another sample of the Al-Fe alloy, heat treated at 1173 K for 2 days and etched with 20 volume percent sulfuric acid solution, was analyzed with the microprobe. In this case the objective of the analysis was to differentiate between two phases with different shades, that is, to determine which phase was $FeAl_2$ and which phase was Fe_2Al_5. Microprobe results showed that the lightly shaded phase was $FeAl_2$ and the darker one was Fe_2Al_5. The η-Fe_2Al_5 phase appeared to have been leached with acid during the etching, that is, aluminum in the surface layer was slightly dissolved, however, the composition of the Fe_2Al_5 phase in the etched sample was the same as in the unetched sample. This indicated that the etching procedure did not affect the composition analysis of the Al-Fe alloy and an etched sample can be used for a microprobe analysis.

An unetched sample of Al-Fe-Mn (59/38/3 wt %) alloy, heat treated at 1173 K for 2 days, was scanned with the microprobe. One hundred points were analyzed along the surface of the alloy with each point 10 microns apart. The averaged composition of the sample was 59.9 wt % of aluminum, 37.0 wt % of iron, and 4.1 wt % of

manganese, which corresponded to the formula, $(Fe,Mn)Al_3$. Microprobe data also showed that the composition of the alloy was quite uniform with no indication of phase segregation.

Activation of Aluminum Alloys

The Al-Fe and Al-Fe-Mn alloys were activated with a NaOH solution to leach out the aluminum from the alloys, making porous and active Raney catalysts with high surface areas. The activation was carried out at various leaching conditions:

Leaching temperature: 298, 323, and 363 K

NaOH concentration: 2 wt %, 10 wt %, and 20 wt %

Activation method: alloy or caustic addition.

The difference between the above two methods was described previously. A special notation was used to identify the Raney catalysts prepared at different leaching conditions as follows: R denotes a Raney catalyst; Fe denotes iron and FeMn denotes iron-manganese catalyst, respectively; A or C indicates that the catalyst was prepared by the alloy addition or the caustic addition method, respectively; numbers following A or C indicate the leaching temperature in degrees centigrade; numbers in parenthesis indicate the concentration of the NaOH solution. If there is no number following the leaching temperature it is an indication that the catalyst had been leached with 20 wt % NaOH solution. As an example, R-FeMn-A50 (10 %) means a Raney iron-manganese catalyst prepared by the alloy addition method at 323 K ($50^{o}C$) with a 10% NaOH solution. R-Fe-C90 means a Raney iron catalyst prepared by caustic addition method at 363 K ($90^{o}C$) with a 20% NaOH solution.

Alloy Addition Method

The percent aluminum leached during the activation process, estimated by hydrogen gas evolution during the leaching process, is presented in Table 4. The extent of aluminum leached increased with increasing leaching temperature and with increasing sodium hydroxide concentration for both Raney Fe and Raney Fe-Mn catalysts irrespective of the preparation method, that is, alloy addition or caustic addition method. The variation of the percent aluminum leached with different leaching temperature for the Al-Fe alloy is presented in Figure 18. The extent of leaching increased with increasing temperature. The Al-Fe alloy obtained from Alpha Products underwent less extensive leaching of the aluminum than the alloy prepared in the laboratory at the same leaching temperature, 363 K. There was a period during which no evolution of hydrogen was observed at the beginning of the leaching period (Figure 18). This phenomenon is apparently related to the presence of aluminum oxide film on the Al-Fe alloy surface. Bernard and Randall[100] observed the same phenomenon during the reaction of aluminum with water and named it the inhibition period. Vedder and Vermilyea[101] called it the induction period. The duration of the induction period increased with decreasing leaching temperature as has been observed by other investigators.[100,101] The dissolution reaction of aluminum does not commence until hydroxyl ion penetrates the oxide film which is broken down during the induction period. The extent of the leaching of aluminum from an Al-Fe-Mn alloy at three different temperatures is presented in Figure 19. The extent of the aluminum leached increased as the leaching temperature increased from 303 to 363 K as expected.

Table 4

Extent of Aluminum Leached

Alloy Addition	Catalyst	% Aluminum Leached	Caustic Addition	Catalyst	% Aluminum Leached
Raney Fe	R-Fe-A25	21.6	Raney Fe	R-Fe-C25	79.9
	R-Fe-A30	55.3		R-Fe-C50	79.1
	R-Fe-A50	73.6		R-Fe-C90	83.7
	R-Fe-A90	89.7		R-Fe-C90[b]	84.5
	R-Fe-A90[a]	85.2		R-Fe-C90 (10%)	43.9
				R-Fe-C90 (2%)	9.2
Raney Fe-Mn	R-FeMn-A30	74.5	Raney Fe-Mn	R-FeMn-C50	85.9
	R-FeMn-A50	90.5		R-FeMn-C50[b]	81.9
	R-FeMn-A90	~100.0		R-FeMn-C90	~100.0
	R-FeMn-A50[a]	80.5			
	R-FeMn-A50(10%)	56.8			

[a]Alloy obtained from Alpha Products.

[b]Duplicate preparation.

Figure 18

Leaching of Aluminum from an Aluminum-Iron Alloy
by Alloy Addition Technique

Sodium Hydroxide Concentration = 20 wt %

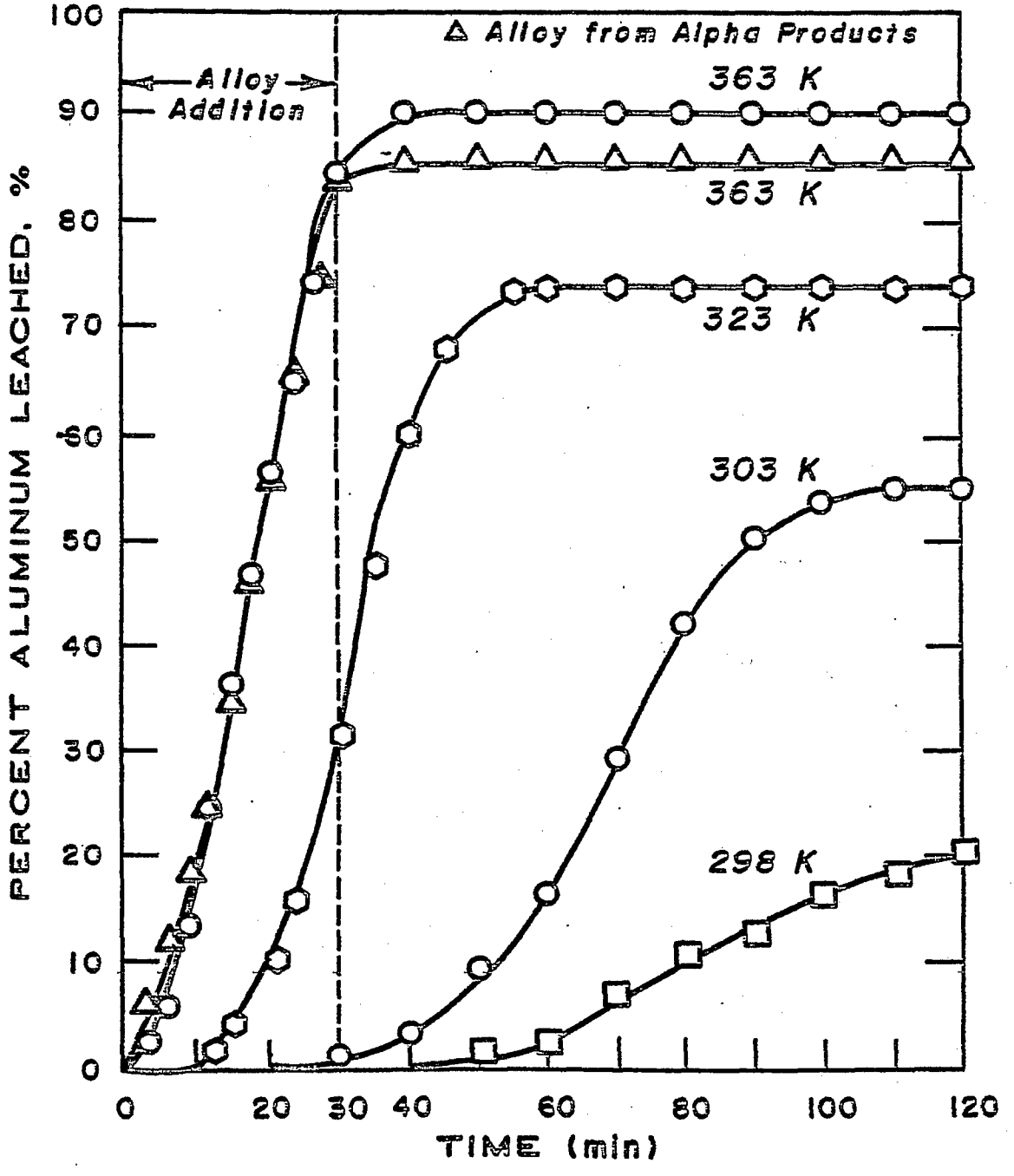
△ Alloy from Alpha Products
Alloy Addition
363 K
363 K
323 K
303 K
298 K
PERCENT ALUMINUM LEACHED, %
TIME (min)
0
10
20
30
40
50
60
70
80
90
100
0
20
30
40
60
80
100
120

Figure 19

Leaching of Aluminum from an Aluminum-Iron-Manganese Alloy by Alloy Addition Technique

Sodium Hydroxide Concentration = 20 wt %

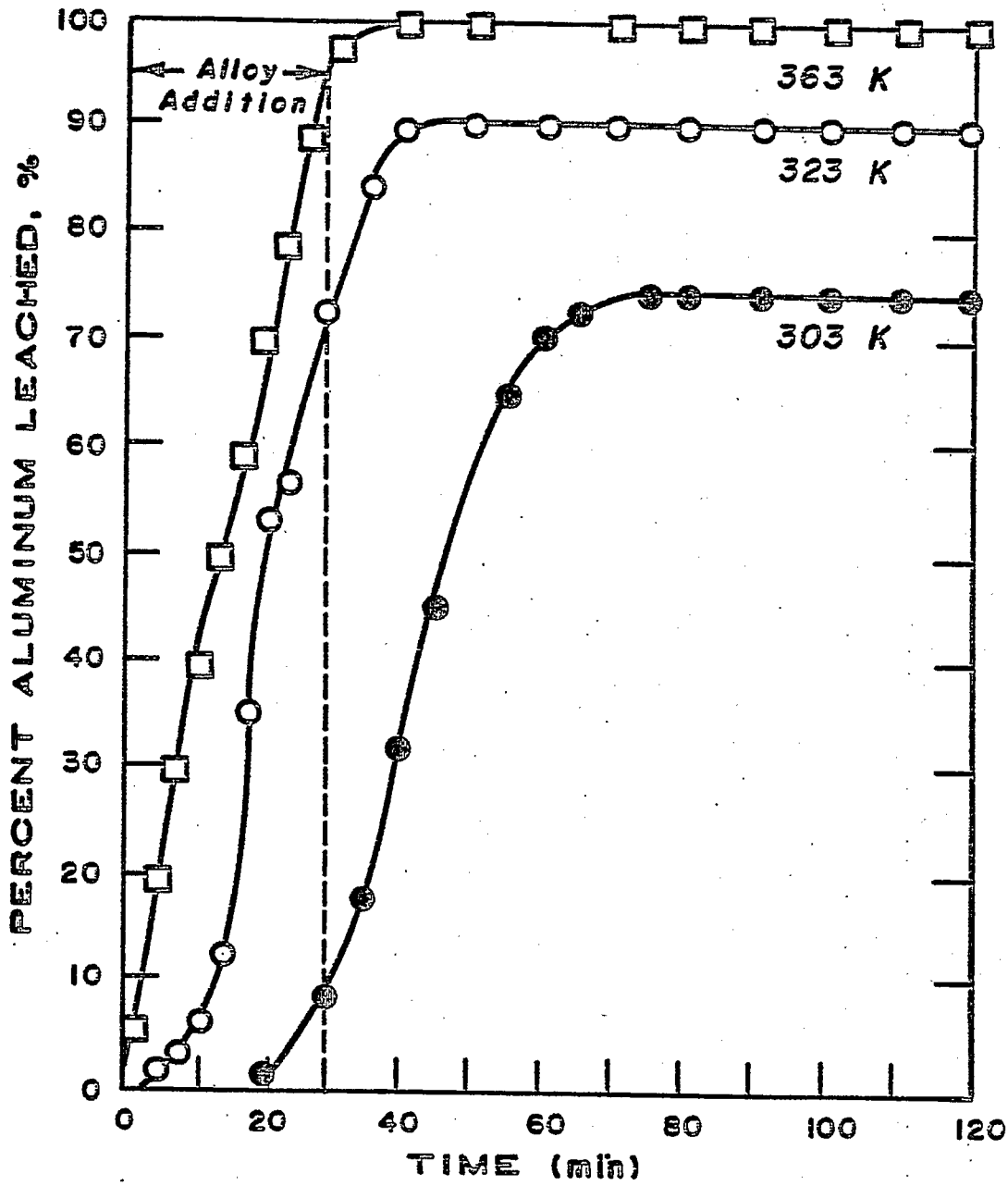
PERCENT ALUMINUM LEACHED, %
TIME (min)
Alloy Addition
363 K
323 K
303 K
0
10
20
30
40
50
60
70
80
90
100
0
20
40
60
80
100
120

An induction period was also observed during the leaching of the Al-Fe-Mn alloy; however, the duration of the induction period was shorter than for the Al-Fe alloy.

The extent of aluminum leached from an Al-Fe-Mn alloy at a single temperature (323 K), but at different catalyst preparation conditions, is presented in Figure 20. The Al-Fe-Mn alloy obtained from Alpha Products was less reactive than the alloy prepared in this laboratory. An activation with 20 wt % NaOH solution resulted in a higher extent of leaching than the activation with 10 wt % solution. The activation with 20 wt % NaOH solution showed shorter induction period than the activation with 10 wt % solution as shown in Figure 20.

Caustic Addition Method

The percent aluminum leached from the Al-Fe alloy at three different temperatures is presented in Figure 21. Two duplicate preparations showed excellent agreement with regard to the extent of aluminum leached at 363 K (Figure 21 and Table 3). Activation at 323 K gave almost the same extent of aluminum leached as the activation at 298 K, however, the extent of aluminum leached was lower than that obtained at 363 K.

A period during which no hydrogen evolution took place was observed after the initial evolution of hydrogen (Figure 21). This phenomenon occurred when the addition of the caustic solution was stopped in order to maintain the leaching temperature constant. This was necessary to avoid an excessive temperature increase due to the highly exothermic nature of the reaction. When the addition of the

Figure 20

Leaching of Aluminum from an Aluminum-Iron-Manganese Alloy by Alloy Addition Technique

Sodium Hydroxide Concentration = 20 wt %;

Temperature = 323 K

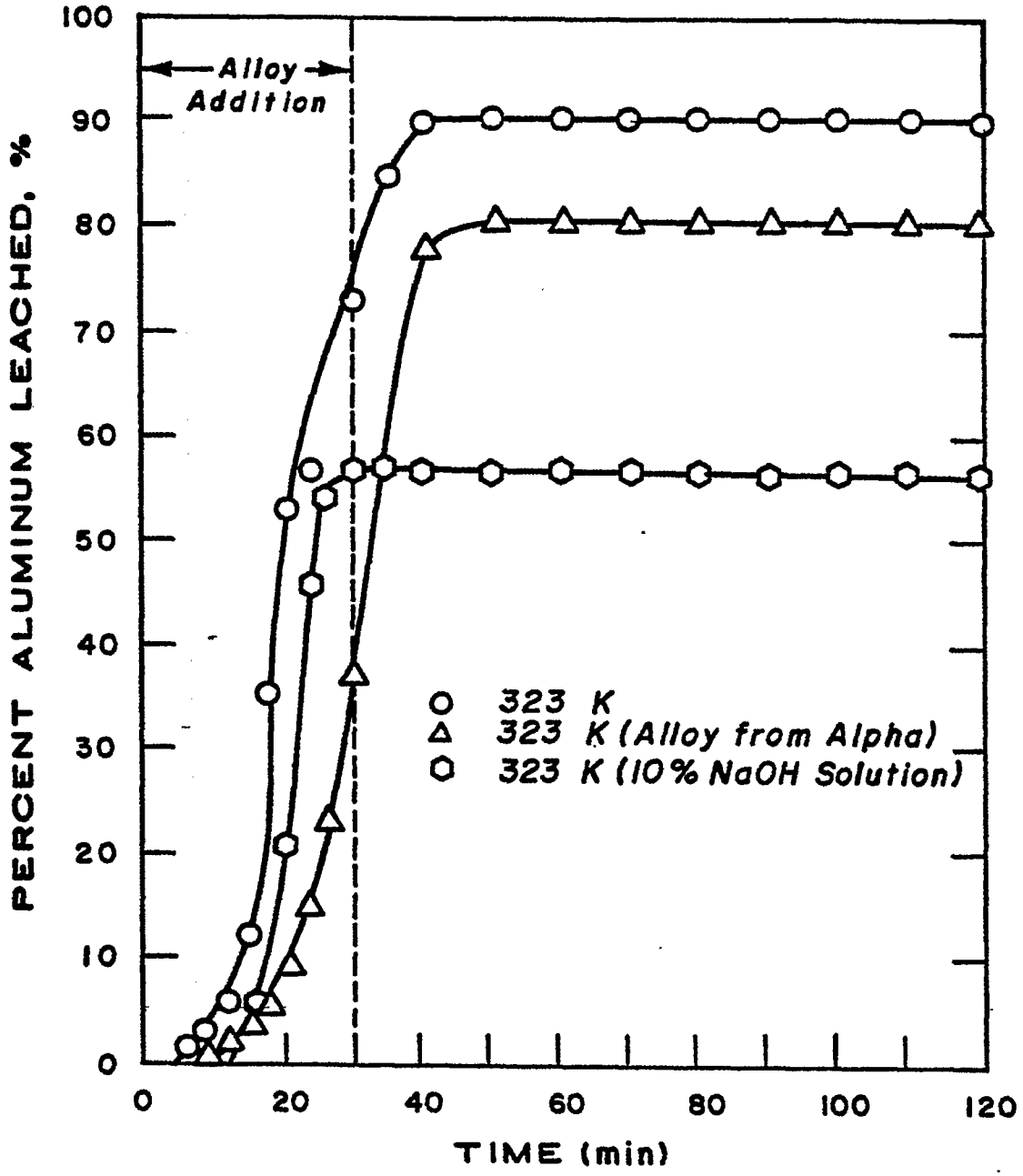
Alloy Addition
PERCENT ALUMINUM LEACHED, %
TIME (min)
323 K
323 K (Alloy from Alpha)
323 K (10% NaOH Solution)
0
10
20
30
40
50
60
70
80
90
100
0
20
40
60
80
100
120

Figure 21

Leaching of Aluminum from an Aluminum-Iron Alloy by Caustic Addition Technique

Sodium Hydroxide Concentration = 20 wt %

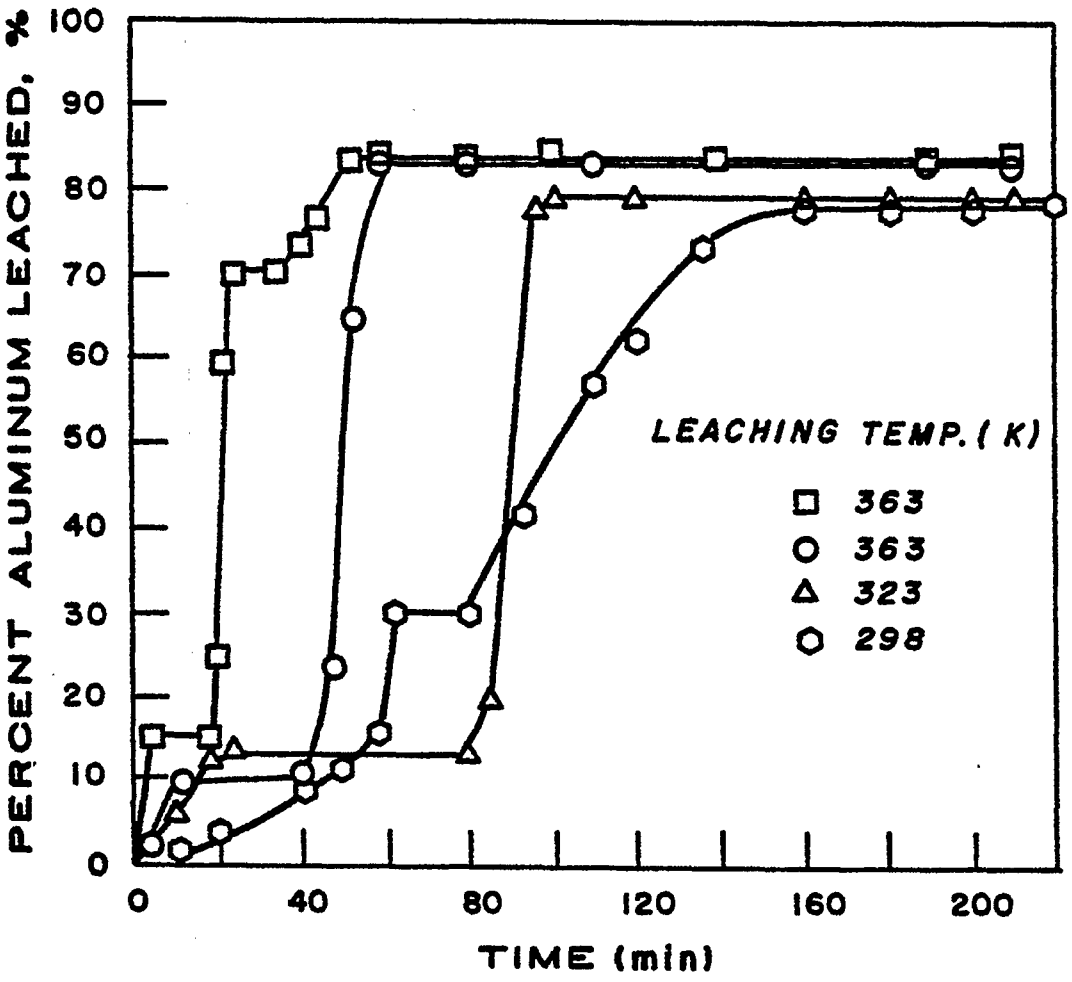
PERCENT ALUMINUM LEACHED, %
100
90
80
70
60
50
40
30
20
10
0
0
40
80
120
160
200
TIME (min)
LEACHING TEMP. (K)
363
363
323
298

caustic solution was stopped, the hydroxyl ion concentration of the solution in the reactor was quite low due to the reaction of the hydroxyl ion with the aluminum. At a pH value below 11 the formation of amorphous aluminum oxide and aluminum hydroxides is favored resulting in a thickening of the oxide or hydroxide layer, which retards or prevents the aluminum dissolution reaction.[101,104] The aluminum dissolution reaction resumes when the hydroxyl ions penetrate the oxide or hydroxide layers or when these layers are dissolved at a high pH value (i.e., after addition of sodium hydroxide solution).

The effect of the concentration of the sodium hydroxide solution at a constant reaction temperature (363 K) on the extent of aluminum leached is presented in Figure 22. The extent of leaching increased as the concentration of the sodium hydroxide solution increased from 2 to 20 wt %.

The leaching of the aluminum from an Al-Fe-Mn alloy at two different temperatures is presented in Figure 23. The extent of leaching was greater at the higher temperature (363 K). The extent of leaching from a duplicate sample of an Al-Fe-Mn alloy at 323 K was quite close to that for the original at 323 K.

Catalyst Characterization

BET Surface Area

The total surface areas of the Raney catalysts have been measured by the BET surface area technique. Mars, et al.[113] reported that the BET surface area of a Raney nickel catalyst stored in water showed a significant decrease with increasing degassing temperature. They ascribed the decrease to the highly exothermic

Figure 22

Leaching of Aluminum from an Aluminum-Iron Alloy
by Caustic Addition Technique

Temperature = 363 K

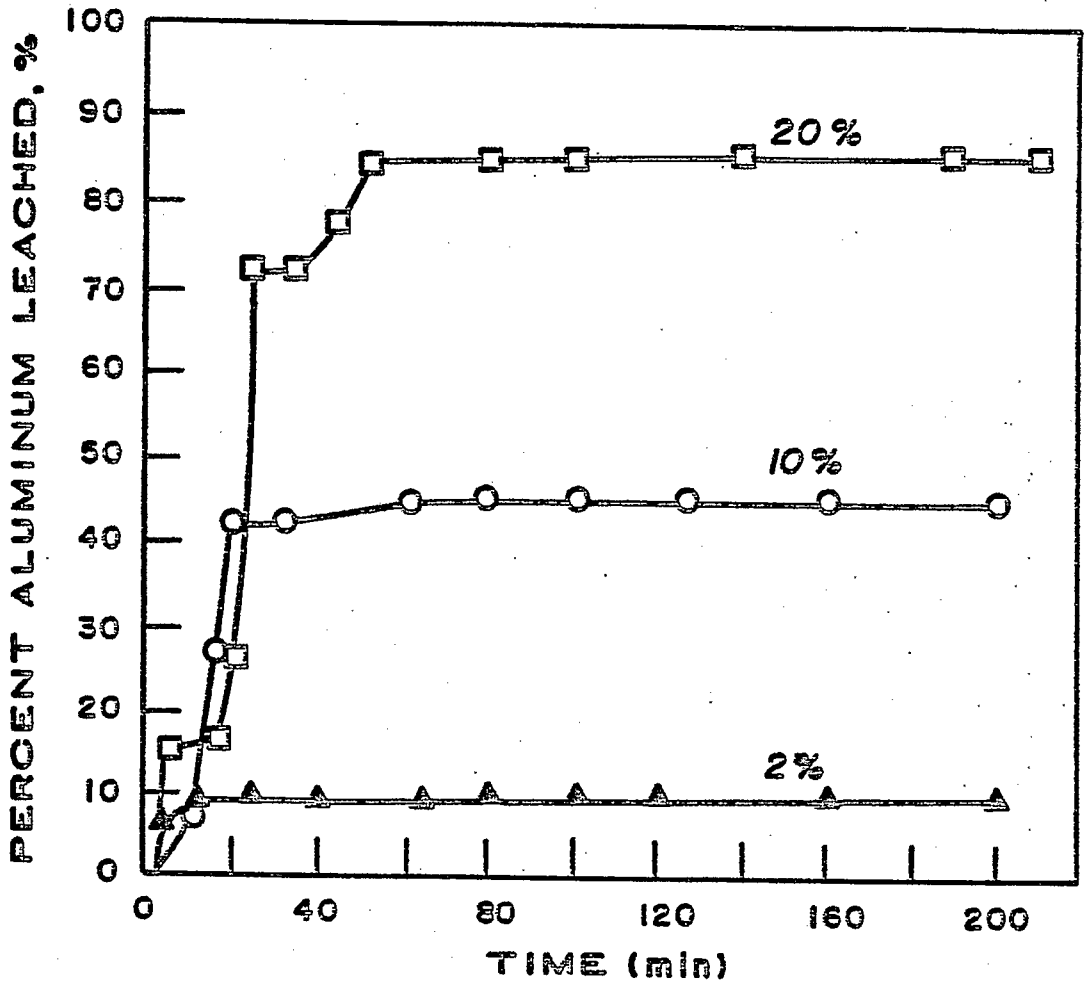
PERCENT ALUMINUM LEACHED, %
100
90
80
70
60
50
40
30
20
10
0
0
40
80
120
160
200
TIME (min)
20%
10%
2%

Figure 23

Leaching of Aluminum from an Aluminum-Iron-Manganese Alloy by Caustic Addition Technique

Sodium Hydroxide Concentration = 20 wt %

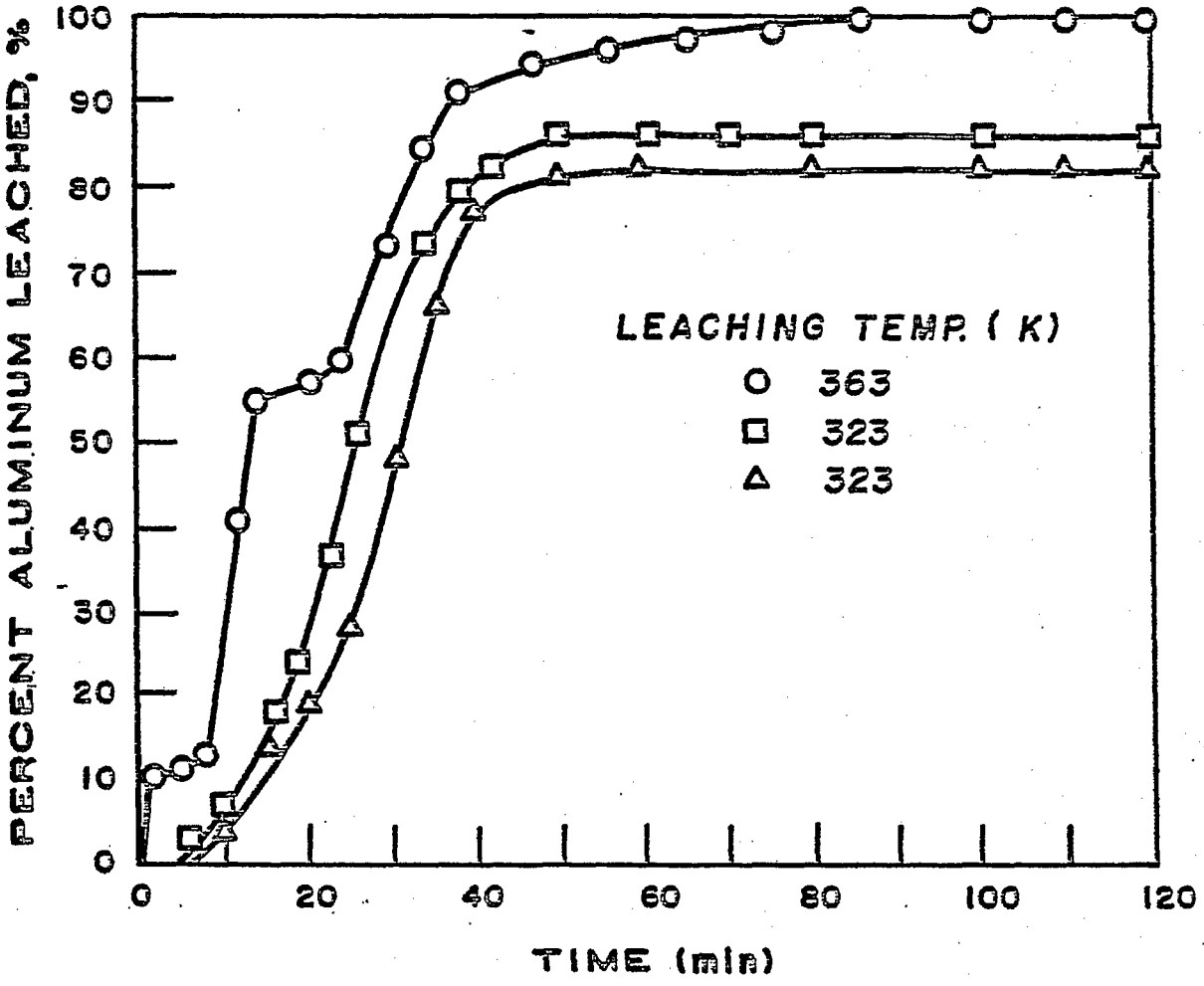
PERCENT ALUMINUM LEACHED, %
100
90
80
70
60
50
40
30
20
10
0
0
20
40
60
80
100
120
TIME (min)
LEACHING TEMP. (K)
363
323
323

reaction of aluminum with residual water remaining in the catalyst pores, resulting in sintering of the catalyst.

The effect of the degassing temperature on the BET surface area has been studied with a Raney iron catalyst (R-Fe-C90), a co-precipitated iron-manganese catalyst, and a precipitated iron catalyst. The Raney iron catalyst was degassed at 353 K for 24 hours and the BET area was determined. The catalyst was then degassed at 393 K for another 24 hours and the surface area was once again determined. This procedure was repeated up to 473 K. Another sample of the same catalyst was degassed at higher temperatures, that is, the initial degassing was done at 523 K, followed by degassing at a progressively higher temperature up to 673 K.

The effect of the degassing temperature on the BET surface area of the Raney iron catalyst (R-Fe-C90) is presented in Table 5 and Figure 24. The surface area of the Raney iron catalyst remained constant after degassing at 393 K and 433 K, however, it decreased after degassing at 473 K. The low surface area after degassing at 353 K appeared to be due to insufficient removal of volatile matter, such as water and ethanol. Degassing at 523 K and above gave essentially the same surface area as degassing at 393 K; however, the surface area decreased by about 10% after degassing at 673 K.

The precipitated catalysts, iron and iron-manganese, were also subjected to the same procedures as the Raney iron catalyst. The degassing was carried out in the temperature range of 393 to 673 K. The effect of degassing temperature on the BET surface areas of the precipitated catalysts, iron and iron-manganese, is presented

Table 5

Effect of Degassing Temperature on BET Surface Area

Catalyst Type	Degassing Temperature (K)	BET Surface Area (m^2/g)
R-Fe-C90	353	46
	393	49
	433	50
	473	43
R-Fe-C90	523	49
	573	48
	623	47
	673	44
Precipitated iron (ppt Fe)	393	232
	473	242
	543	233
	603	214
	673	152
Coprecipitated iron-manganese (coppt Fe-Mn)	393	242
	473	244
	543	237
	603	221
	673	203

Figure 24

Effect of Degassing Temperature on
BET Surface Area

Catalyst: R-Fe-C90

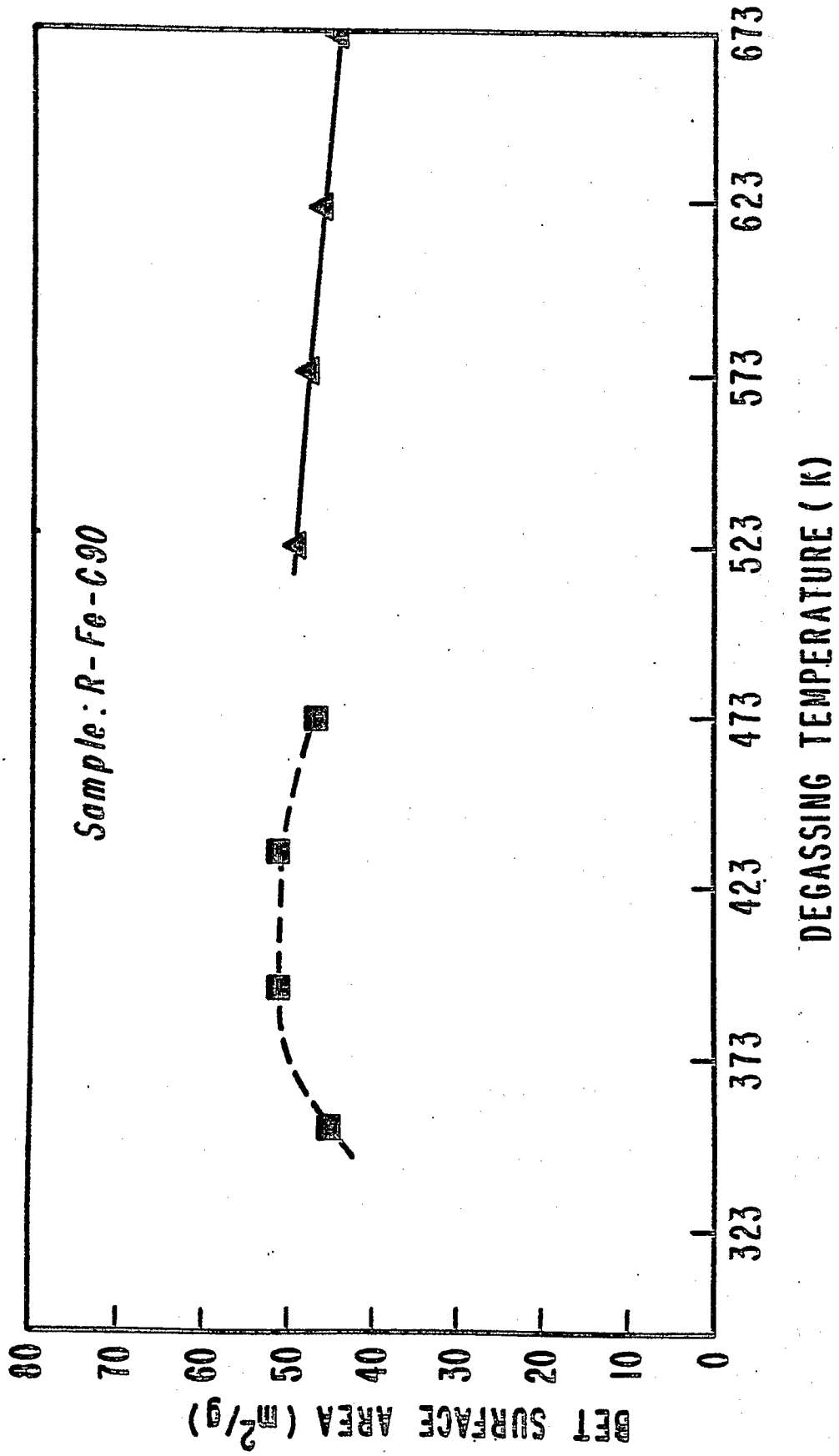
Sample: R-Fe-C90
BET SURFACE AREA (m^2/g)
0
10
20
30
40
50
60
70
80
323
373
423
473
523
573
623
673
DEGASSING TEMPERATURE (K)

in Table 5 and Figure 25. The surface areas of the precipitated Fe and coprecipitated Fe-Mn catalysts showed a noticeable decrease after degassing at 603 K and above as indicated in Figure 25.

These experiments indicated that degassing the catalyst at 393 K for 24 hours seems to be proper for both the Raney and the precipitated type catalysts to obtain representative surface areas without altering the surface structure significantly.

The surface area data for the Raney iron catalyst (Table 5) indicates that the catalyst was not affected by the degassing temperature. Freel, et al.[115] also found that the surface area of a Raney nickel catalyst, stored under absolute ethanol, remained constant irrespective of degassing at different temperatures except for degassing below 393 K. A sharp decrease in surface area of a Raney nickel with increasing degassing temperature observed by Mars, et al.[113] seemed to be due to the relatively abundant residual water remaining in the catalyst compared to the Raney nickel catalyst stored under absolute ethanol. All the catalysts have been degassed at 393 K for 24 hours just prior to each BET surface area measurement. The BET surface area data is presented in Table 6. The surface area of the Raney iron catalyst prepared with 20 wt % NaOH solution ranged from 41 to 54 m^2/g, depending on the preparation temperature. The only exceptions were the Raney iron catalysts, prepared at 363 K by the alloy addition method, R-Fe-A90, for which the surface areas were 26 m^2/g and 29 m^2/g, depending on the source of the Al-Fe alloy used. No trend or correlation could be found between the surface area of the Raney iron catalyst and the preparation conditions such as leaching temperature.

Figure 25

Effect of Degassing Temperature on
BET Surface Area

Catalyst: Precipitated Fe and
Coprecipitated Fe-Mn

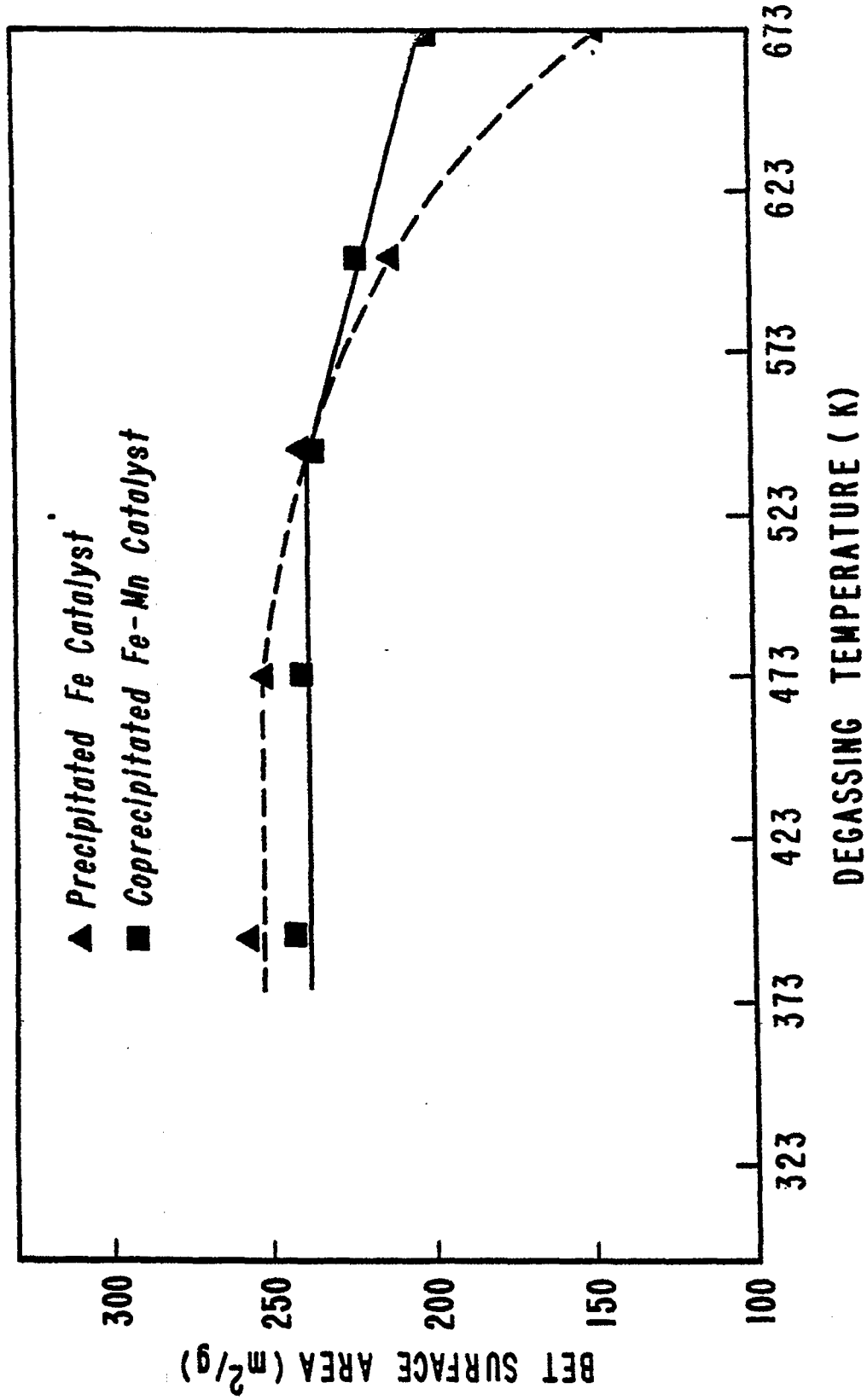
▲ Precipitated Fe Catalyst
■ Coprecipitated Fe-Mn Catalyst
BET SURFACE AREA (m^2/g)
300
250
200
150
100
323
373
423
473
523
573
623
673
DEGASSING TEMPERATURE (K)

Table 6

BET Surface Area

Catalyst Type	Catalyst	BET Area (m^2/g)	Catalyst Type	Catalyst	BET Area (m^2/g)
Raney Fe	R-Fe-A25	46	Raney Fe-Mn	R-FeMn-A30	65
	R-Fe-A30	51		R-FeMn-A50	64
	R-Fe-A50	46		R-FeMn-A50[a]	68
Alloy Addition	R-Fe-A90	26	Alloy Addition	R-FeMn-A90	81
	R-Fe-A90[a]	29		R-FeMn-A50 (10%)	39
Raney Fe	R-Fe-C25	54	Raney Fe-Mn	R-FeMn-C50	78
	R-Fe-C50	41	Caustic Addition	R-FeMn-C90	116
	R-Fe-C50[b]	45			
Caustic Addition	R-Fe-C90	49	Precipitated	ppt Fe	232
	R-Fe-C90[b]	50		coppt Fe-Mn	242
	R-Fe-C90 (10%)	39			
	R-Fe-C90 (2%)	8			

[a]Alloy from Alpha Products.

[b]Duplicate preparation

The surface areas of Raney iron-manganese catalysts were higher (64 - 116 m^2/g) than the surface areas of the Raney iron catalysts (26 - 54 m^2/g). This difference may be due to the differences in alloy type and compositions. In the case of the Raney Fe-Mn catalyst a high leaching temperature, generally, yielded a catalyst with large surface area.

At the same leaching temperature lower concentration of the sodium hydroxide solution produced a catalyst with lower surface area, when compared to the catalyst prepared with 20 wt % NaOH solution as can be seen from the surface area of R-Fe-C90 (10%), R-Fe-C90 (2%), and R-FeMn-A50 (10%) in Table 6. This can be explained by a low extent of aluminum leached with the low concentrations of sodium hydroxide solution (10 or 2%) during the leaching process. Thereby, the development of pore structure is rather incomplete, yielding a low surface area catalyst. The precipitated catalysts as prepared had much higher surface area than the Raney catalysts (Table 6).

X-Ray Diffraction

The Raney catalysts were characterized by x-ray powder diffraction to identify the metal phases present in the catalyst and to estimate the crystallite size of the catalyst.

Phase identification. The metal phases identified are listed in Table 7. Alpha-iron phase was identified in all of the Raney iron and Raney iron-manganese catalysts. Magnetite (Fe_3O_4) was identified in catalysts activated at 363 K by the caustic addition method, however, catalysts (Raney Fe and Fe-Mn) activated

Table 7

Results of X-Ray Diffraction Study

Catalyst	Phases	Crystallite Size (Å)
R-Fe-A90	α-Fe	252
R-Fe-A50	α-Fe	126
R-Fe-A30	α-Fe, Fe-Al Alloy	--
R-Fe-A25	α-Fe, Fe-Al Alloy	--
R-Fe-A90[a]	α-Fe	222
R-Fe-C90	α-Fe, Fe_3O_4	182
R-Fe-C50	α-Fe	149
R-Fe-C25	α-Fe, Fe-Al Alloy	--
R-Fe-C90 (10%)	α-Fe, Fe-Al Alloy Fe_3O_4	--
R-Fe-C90 (2%)	α-Fe, Fe-Al Alloy	--
R-FeMn-A90	α -Fe	107
R-FeMn-A50	α -Fe	93
R-FeMn-A30	α -Fe, Fe-Al-Mn Alloy	--
R-FeMn-A50[a]	α -Fe	74
R-FeMn-A50 (10%)	α -Fe, Fe-Al-Mn Alloy	--
R-FeMn-C90	α -Fe, Fe_3O_4	93
R-FeMn-C50	α -Fe	74
ppt Fe	α -Fe_2O_3	--
Coppt Fe-Mn	α -Fe_2O_3, Mn_3O_4	--

[a]Alloy from Alpha Products.

at the same temperature by the alloy addition method did not have any magnetite phase. The magnetite must have been formed from α-Fe by an oxidation reaction during the leaching period. The Raney catalysts prepared at a low temperature (298 K) or with low concentrations of sodium hydroxide solution (2 wt % and 10 wt %) contained unreacted aluminum alloy phases in addition to the α-Fe phase (Table 7). Schwarzendruber and Evans[109] also found that a Raney iron catalyst contained both α-Fe and magnetite phases when an aluminum-iron alloy (50/50 wt %) was activated with a 25 wt % NaOH solution at 353 K and above. No magnetite was found in catalysts leached at or below 343 K and iron hydroxide, $Fe(OH)_2$, was identified in the catalysts prepared at low temperatures (273 K and 298 K) in addition to an aluminum-depleted aluminum-iron alloy and α-Fe phases.[109] No $Fe(OH)_2$ could be identified in this study due to its lack of crystallinity.

The x-ray diffraction patterns of the Raney catalysts showed a gradual depletion of the alloy phases and a more distinct appearance of the α-Fe phase as the alloy activation temperature increased (Figure 26). Robertson and Anderson[107] and Dirksen and Linden[17] identified gibbsite (α-$Al_2O_3 \cdot 3H_2O$) or bayerite (β-$Al_2O_3 \cdot 3H_2O$) in Raney nickel catalysts activated at 353 K with a 2 wt % NaOH solution. No such aluminum hydroxide could be detected in a Raney iron catalyst activated at 363 K with a 2 wt % solution [R-Fe-C90 (2%)]. The extent of aluminum leached, monitored by hydrogen gas evolution, was only 9% in the case of Al-Fe alloy under the above leaching conditions, while the Al-Ni alloy (50/50 wt %) was reported to have had more than 90% of the aluminum leached under a similar condition.

Figure 26

X-Ray Diffraction Pattern of Raney Iron Catalysts

A: Al-Fe Alloy Phase

F: α-Fe

M: Magnetite

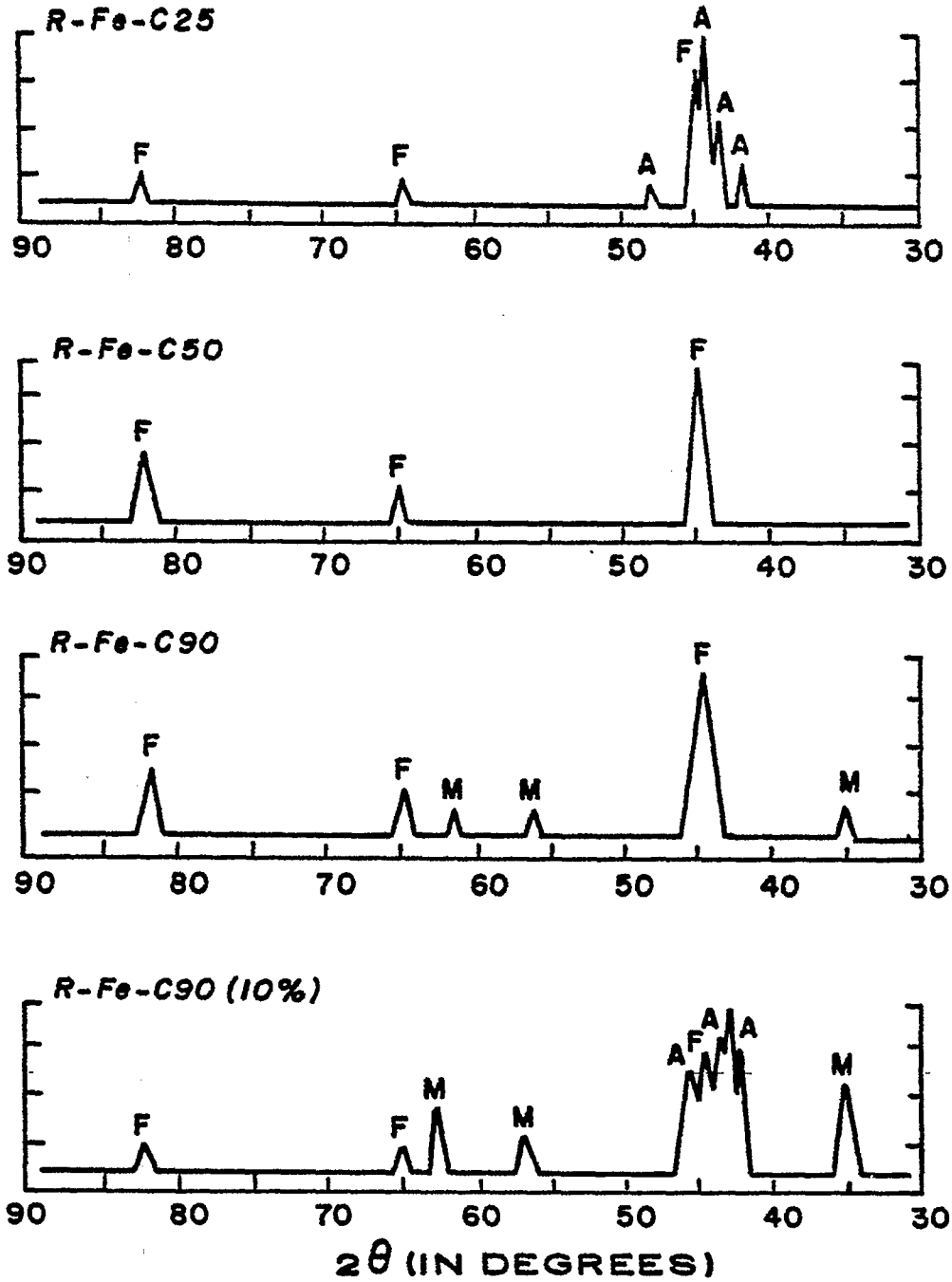
R-Fe-C25
F
F
A
F
A
A
90
80
70
60
50
40
30
R-Fe-C50
F
F
F
90
80
70
60
50
40
30
R-Fe-C90
F
F
M
M
F
M
90
80
70
60
50
40
30
R-Fe-C90 (10%)
F
F
M
M
A
F
A
A
M
90
80
70
60
50
40
30
2θ (IN DEGREES)

The significant differences in the reactivity for the aluminum dissolution reaction between the two types of alloys may be due to different crystal structures. At such a low extent of aluminum leached from an Al-Fe alloy (9%), the gibbsite or bayerite may not have been formed to an appreciable amount to be detected by x-ray diffraction.

The precipitated catalysts (Fe and Fe-Mn) showed very broad and diffuse x-ray peaks, indicating incomplete crystallization during the catalyst preparation. The diffraction pattern of precipitated iron catalyst indicated the presence of hematite (α-Fe_2O_3), while the coprecipitated Fe-Mn indicated the presence of hausmannite (Mn_3O_4) in addition to the hematite phase.

It is noteworthy that none of the Raney iron-manganese catalysts indicated the presence of a manganese-containing phase, such as manganese oxide or manganese metal, although the manganese contents of the two types of the catalyst, coprecipitated and Raney, were almost the same. This indicated that the Mn atoms in the Raney Fe-Mn catalyst were incorporated into the α-Fe crystal lattice and did not form a separate manganese-containing phase.

Determination of crystallite size. The crystallite size of the α-Fe in the Raney catalyst was estimated from the line broadening of a diffraction peak at the (110) plane of the α-Fe, using the Scherrer equation.[50] The Scherrer equation is regarded to give a relatively accurate measure of a crystallite size, especially for a group of catalysts prepared by the same procedures such as the Raney catalysts used in this investigation.

Since the Al-Fe and Al-Fe-Mn alloys both have intense reflections near the diffraction peak of α-Fe at (110) plane, the above estimate could not be made for the catalysts which contained some remaining alloy phases due to the overlapping of the diffraction peaks. This was the case for catalysts prepared below 323 K or prepared with low concentrations of NaOH solution (< 20%).

The crystallite size of the Raney catalyst is also presented in Table 7. From the table it can be seen that a high temperature (363 K) leaching produced a catalyst with a larger crystallite size compared to the one prepared at a lower temperature (323 K), when the other preparation conditions were the same. The effect of the leaching temperature on the crystallite size was most pronounced in the case of Raney iron catalyst prepared by the alloy addition method. A difference of 40 K in leaching temperature resulted in a difference in crystallite size of about two times. The change in crystallite size with increasing leaching temperature was quite consistent with observations made by Robertson and Anderson[107] who found that a lower temperature or a shorter leaching time produced a nickel catalyst with a smaller crystallite size. The crystallite size of the Raney catalyst ranged quite widely from 70 Å to 250 Å, while it ranged from 35 to 60 Å in the case of Raney nickel catalyst.

The Raney catalysts prepared from Alpha Products alloys had smaller crystallite size than the Raney catalysts prepared from alloys made in this laboratory at the same preparation conditions.

Robertson and Anderson[107] correlated the BET surface area of Raney nickel catalyst with the crystallite size of the nickel,

measured by the x-ray line broadening technique using an equation suggested by Allred, et al.:[159]

$$S = \frac{K f 10^4}{L d} \qquad (70)$$

where S is the surface area (m^2/g), K is the geometric factor equal to 6 for spherical or cubic crystallites, f is the fraction of crystallite surface available for gas adsorption, d is the density (g/cm^3), and L is the mean size of crystallite ($\mathring{A}$). The surface areas and the reciprocals of the crystallite size for the Raney catalysts are listed in Table 8. A reasonable linear relationship existed between the BET surface area and the reciprocal of the crystallite size as illustrated in Figure 27. The f value was calculated from the slope of the plot in Figure 27, using K = 6 and d = 7.86 for the body-centered cubic crystals of α-Fe. The real density of the α-Fe in the Raney catalyst may be lower than 7.86.

The f value obtained was 0.63, which is quite close to 0.65 for Raney nickel catalyst with face-centered cubic structures obtained by Robertson and Anderson.[107]

Atomic Absorption

The elemental compositions and the extent of aluminum leached as determined by atomic absorption are listed in Table 9 for the Raney iron-manganese catalysts and in Table 10 for the Raney iron catalysts, respectively. The tables also include the extent of aluminum leached and the elemental compositions of the catalysts as estimated by hydrogen evolution.

Table 8

BET Surface Area and Crystallite Size

Catalyst	L, Crystallite Size (Å)	$\frac{1}{L} \times 10^3$ ($Å^{-1}$)	BET Surface Area (m^2/g)
R-Fe-A50	126	7.93	46
R-Fe-A90	252	3.97	26
R-Fe-A90[a]	222	4.50	29
R-Fe-C50	149	6.73	41
R-Fe-C90	182	5.49	49
R-FeMn-A50	93	10.77	64
R-FeMn-A90	107	9.36	81
R-FeMn-A50	74	13.57	68
R-FeMn-C50	74	13.57	78

[a]Alloy from Alpha Products.

Figure 27

Correlation of BET Surface Area
and Crystallite Size

Catalyst: Raney Iron and Iron-Manganese

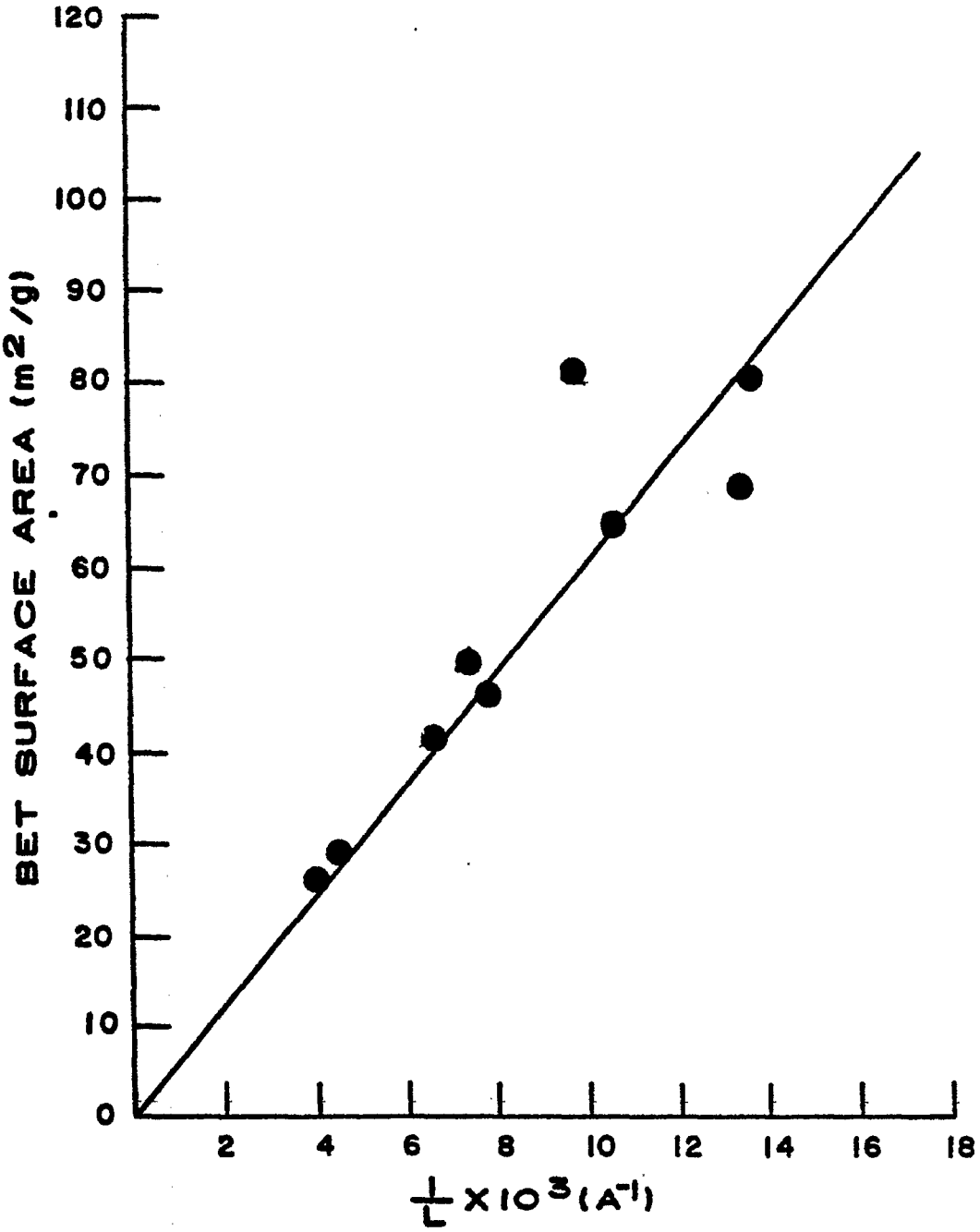
BET SURFACE AREA (m2/g)
120
110
100
90
80
70
60
50
40
30
20
10
0
2
4
6
8
10
12
14
16
18
1/L x 10^3 (A^-1)

Table 9

Composition of Raney Iron-Manganese Catalysts

Catalyst	Elemental Analysis						Percent Aluminum Leached		Fe/Mn Ratio
	Atomic Absorption (wt %)			Hydrogen Evolution (wt %)					
	Fe	Al	Mn	Fe	Al	Mn	A.A.	H_2	
R-FeMn-A30	66.0	29.9	4.1	67.8	26.8	5.4	71.9	74.5	16.10
R-FeMn-A50	90.0	3.7	6.3	81.5	12.0	6.4	97.9	90.5	14.29
R-FeMn-A90	89.6	3.6	6.7	92.7	0	7.3	97.6	100	13.37
R-FeMn-A50[a]	91.6	2.7	5.7	72.4	21.9	5.7	99.2	80.5	16.07
R-FeMn-A50 (10%)	61.7	34.2	4.2	57.2	38.3	4.5	65.1	56.8	14.69
R-FeMn-C50	90.9	3.5	5.6	77.0	16.8	6.1	98.6	85.9	16.23
R-FeMN-C90	89.8	3.5	6.7	92.7	0	7.3	97.8	100	13.40
Al-Fe-Mn Alloy	38.1 (38.0)	58.7 (59.8)	3.2 (3.0)						11.91 (12.67)
Coppt Fe-Mn	95.5 (95.3)	--	4.5 (4.7)						

[a]Alloy from Alpha Products.

Table 10

Composition of Raney Iron Catalysts

Catalyst	Elemental Analysis: Atomic Absorption (wt %) Fe	Atomic Absorption (wt %) Al	Hydrogen Evolution (wt %) Fe	Hydrogen Evolution (wt %) Al	Percent of Aluminum Leached: A.A.	Percent of Aluminum Leached: H_2
R-Fe-A25	77.4	22.6	56.1	43.9	70.8	21.6
R-Fe-A30	86.1	13.9	69.0	31.0	83.9	55.3
R-Fe-A50	87.4	12.6	79.0	21.0	85.6	73.6
R-Fe-A90	98.2	1.8	90.7	9.3	98.2	89.7
R-Fe-A90[a]	95.4	4.6	87.0	13.0	95.2	85.2
R-Fe-C25	83.0	17.0	83.0	17.0	79.5	79.7
R-Fe-C50	90.6	9.4	83.0	17.0	89.6	79.1
R-Fe-C90	93.3	6.7	86.0	14.0	92.8	83.7
R-Fe-C90 (10%)	72.1	27.9	64.0	36.0	61.3	43.9
R-Fe-C90 (2%)	56.8	43.2	52.4	47.6	23.9	9.2

[a]Alloy from Alpha Products.

The elemental compositions of the Raney iron-manganese catalysts obtained by the two methods show reasonable agreements except for the catalyst R-FeMn-A50, prepared from an Al-Fe-Mn alloy furnished by Alpha Products. This catalyst was not completely dissolved even with concentrated hydrochloric acid solution in the preparation of the atomic absorption sample solution, leaving some white precipitation, which appeared to be aluminum oxide. The iron/manganese ratios (weight basis) for all the Raney iron-manganese catalysts were higher than the ratio for the original alloy, 11.91. This indicated that some of the manganese atoms were removed during the dissolution of aluminum with the NaOH solution, since iron atoms are not dissolved in alkaline solution. Approximately 20% of the manganese atoms were removed during the activation process. Russel, et al.[15] also reported that manganese atoms were partially dissolved during the leaching of an aluminum alloy containing manganese with sodium hydroxide solution.

The extent of aluminum leached calculated from atomic absorption analysis, generally gave higher values, when compared to the value obtained from hydrogen evolution. One of the plausible explanations for this observation is the retention of a large volume of hydrogen gas in the Raney catalysts, which may account for as much as 5% error in the volume of hydrogen evolved (and also in the extent of aluminum leached) based on the fact that the Raney catalyst may contain as much as 30 cm^3 (STP) hydrogen per gram of metal.[113,132] The extent of aluminum leached based on the atomic absorption analysis was calculated assuming neither iron nor

manganese was dissolved with NaOH solution during the activation period.

The composition of the aluminum-iron-manganese alloy was determined by atomic absorption analysis to check the accuracy of the atomic absorption technique. The numbers in parentheses are the actual compositions of the metal elements. There is an excellent agreement between the two sets of values.

The composition of the coprecipitated iron-manganese catalyst was determined and was compared to the values in the parentheses, which was the actual composition of the catalyst during the mixing of two metal components when preparing the catalyst. Two sets of data showed good agreement indicating that all the metal ions (iron and manganese) were completely precipitated during the catalyst preparation.

The elemental composition of the Raney iron catalysts as determined by atomic absorption analysis as well as those estimated from the hydrogen evolution data are presented in Table 10. Generally, there is reasonable agreement between the two sets of data, except for the catalysts R-Fe-A25 and R-Fe-A30. The large discrepancy in aluminum contents for these two catalysts seems to be due to the reaction of residual aluminum with water during the washing of the catalysts in water. Continued evolution of hydrogen was observed during the washing of the two catalysts, indicating that some portion of the remaining aluminum was dissolved out.

Thermogravimetric Reduction Study

Precipitated Catalyst

A series of catalyst reduction studies have been carried out with a coprecipitated iron-manganese catalyst (Mn/Fe = 5/100 atomic ratio) using a DuPont TGA Model 951 and a Perkin-Elmer TGS-2 system.

The weight loss curve for the coprecipitated catalyst while heating to 773 K in flowing helium at two different heating rates (0.5 and 2 K/min) is presented in Figure 28. Heating the catalyst at the slower rate (0.5 K/min) resulted in a more complete removal of the volatile matter, water, or residual NO_3^- ion that remained in the catalyst after the washing process. The catalyst did not lose additional weight even after prolonged heating at 773 K. The derivative of the weight change with respect to temperature is shown in the lower curve in Figure 28. The derivative curve revealed that a significant weight change took place at about 533 K. The effect of different heating rates on the catalyst weight loss in flowing hydrogen is shown in Figure 29. All three heating rates (0.5, 2.0, and 5.0 K/min) resulted in the same final weight loss, 35.4 wt %. After heating in hydrogen to 773 K, the catalyst sample was cooled to room temperature in flowing hydrogen. The sample was flushed with helium gas at room temperature and air was introduced into the furnace chamber. The sample was heated to 773 K in flowing air at the same heating rate, 0.5 K/min, for all three cases.

The catalysts which were heated in hydrogen at heating rates of 0.5 and 2 K/min gained weight. The weight gained corresponded to the final weight of the catalyst obtained after heating under helium, that is, 9.4% lower than the original weight. However, a sample

Figure 28

Temperature Programmed Thermal Analysis (TGA) Curves

Coprecipiteted Iron-Manganese Catalyst;

Helium Atmosphere

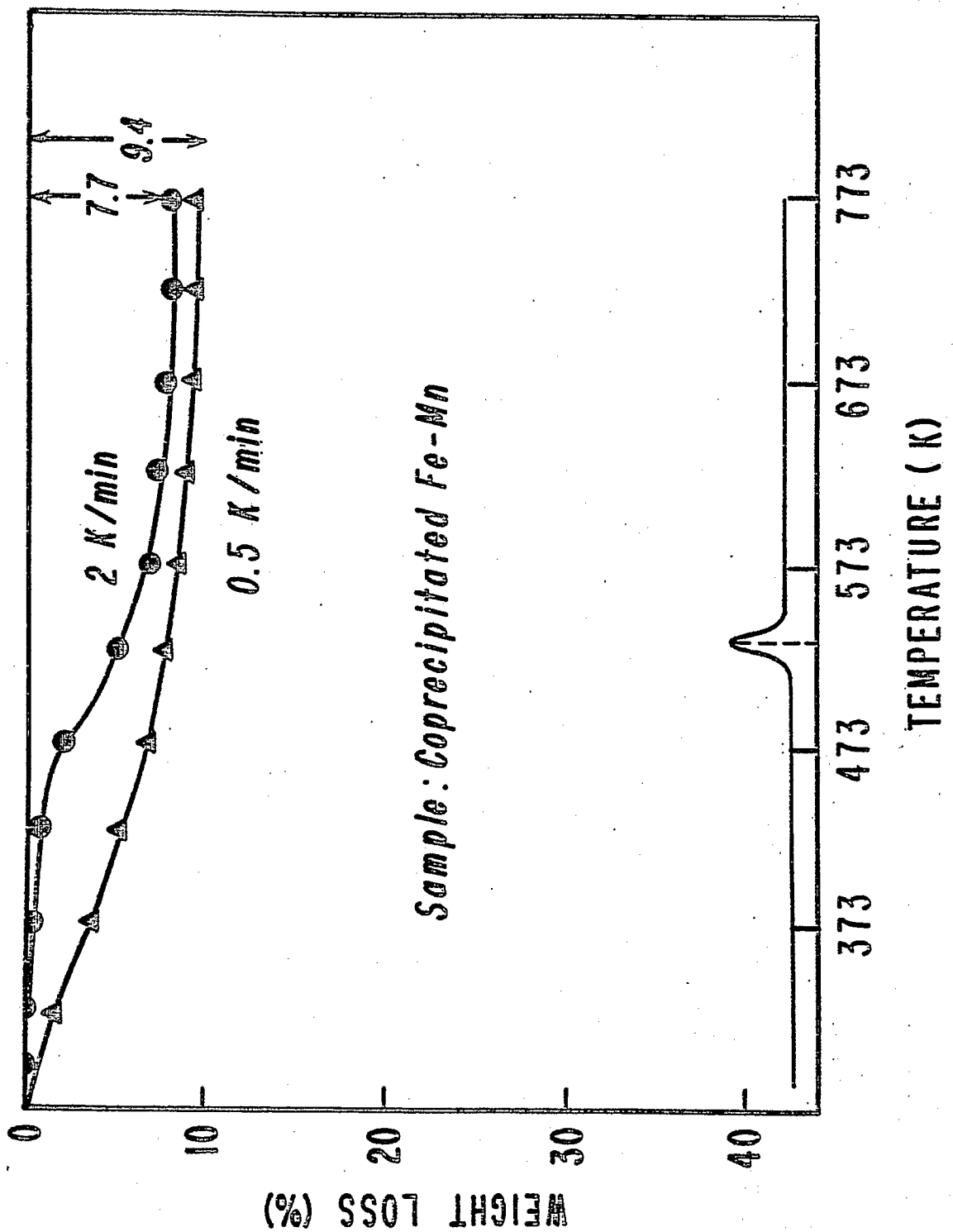
WEIGHT LOSS (%)
0
10
20
30
40
373
473
573
673
773
TEMPERATURE (K)
Sample : Coprecipitated Fe-Mn
2 K/min
0.5 K/min
7.7
9.4

Figure 29

Temperature Programmed Thermal Analysis (TGA) Curves

Coprecipitated Iron-Manganese Catalyst;

Hydrogen/Helium/Air Atmosphere

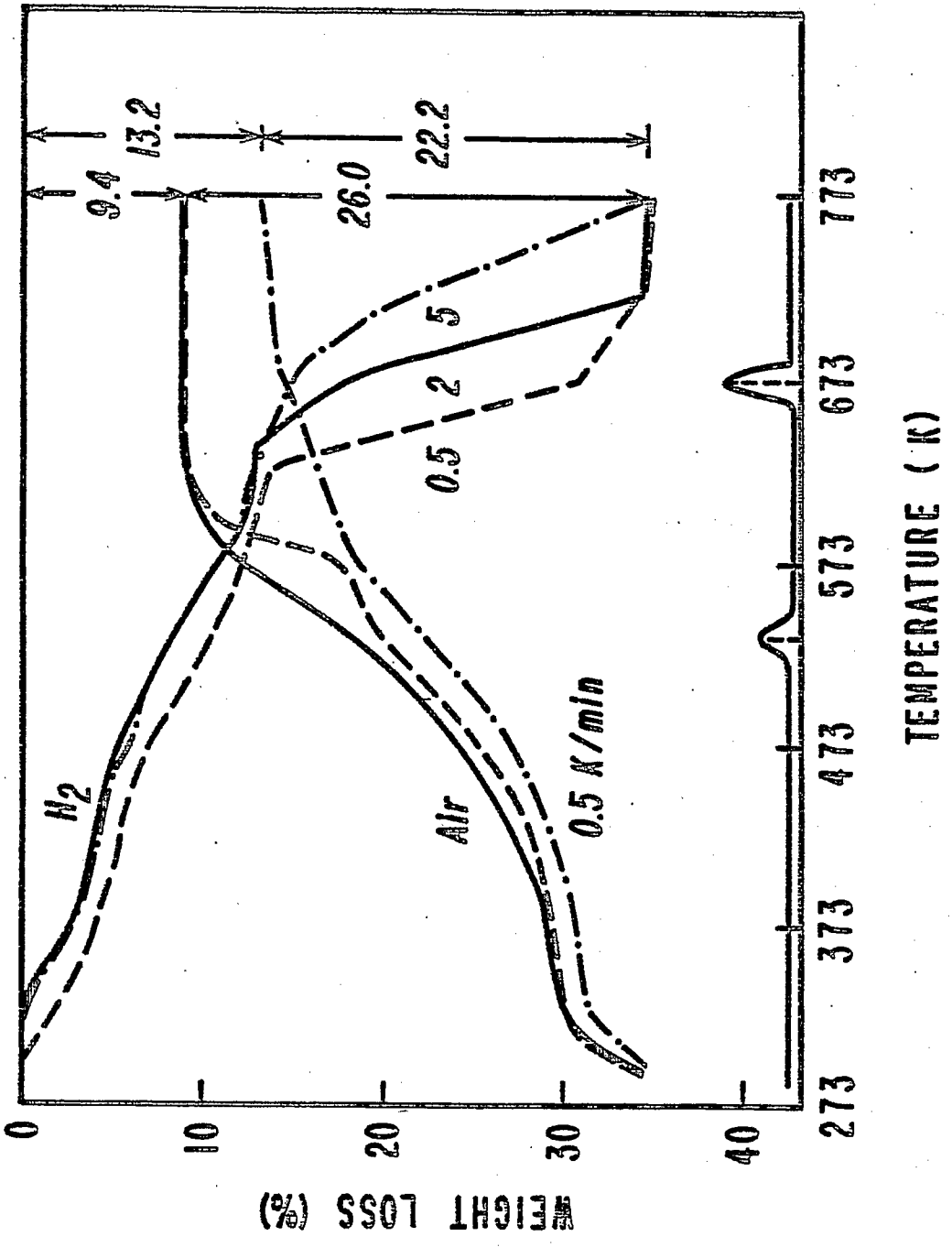
WEIGHT LOSS (%)
0
10
20
30
40
TEMPERATURE (K)
273
373
473
573
673
773
9.4
13.2
26.0
22.2
H_2
Air
0.5 K/min
0.5
2
5

heated at a heating rate of 5 K/min, gained less weight than the above two samples, that is, 13.2% below the original weight. This experiment indicated that the reduction-oxidation cycle was irreversible when the heating rate during the reduction in hydrogen was too high, 5 K/min. The irreversibility may be due to sintering of the crystallites or to changes in pore structure of the catalyst when the catalyst was reduced at the high heating rate.

The final weight loss after reduction was 35.4 wt %. Subtracting the 9.4% loss due to volatile matter, the weight loss due to reduction was 26.0 wt %. The reduction weight loss, based on the catalyst weight on a volatile-matter free basis, was 28.70 wt %. The extent of reduction of the catalyst during the above reduction was estimated from the previous weight loss data, based on the expected weight loss after a complete reduction. The catalyst was shown to consist of Fe_2O_3 and Mn_3O_4 from the x-ray diffraction study and the atomic ratio of Mn/Fe was 5/100. The weight loss after complete reduction was:

$$\frac{3 \times A.W.(O)}{M.W.(Fe_2O_3)} \times \frac{100}{105} + \frac{4 \times A.W(O)}{M.W.(Mn_3O_4)} \times \frac{2}{3} \times \frac{5}{105} = 0.2951 \quad .$$

A.W. (O) refers to atomic weight of oxygen atom and M.W. (compound) refers to molecular weight of the compound in the parenthesis. The extent of reduction was:

$$\frac{0.2870}{0.2951} \times 100 = 97 \ (\%) \ .$$

The calculation shows that the catalyst underwent an essentially complete reduction during the reduction period. There were two

temperatures at which significant weight changes took place, 533 K and 673 K. The first weight change at 533 K was also observed when the catalyst was heated in helium (Figure 28). The second weight change at 673 K must be due to the reduction of iron oxide to iron. It can be concluded that a heating rate of 2 K/min during the reduction of the coprecipitated catalyst is the proper value to prevent any significant changes in catalyst structure or surface area and to permit nearly complete reduction.

A series of isothermal runs were made to determine an optimum reduction temperature for the coprecipitated catalyst. Since the DuPont TGA 951 was not capable of a combined operation in which programmed heating is followed by isothermal heating period in a single run, the catalyst was heated in a series of isothermal steps with a 50 K difference between two adjoining steps to minimize any adverse effects of a rapid heating rate.

The sample was heated to 393 K and the temperature was maintained at this point until there was no further weight change. The temperature was then increased to 443 K and was maintained at 443 K until there was no further weight change. This procedure was repeated until the final temperature, 773 K, was reached. The total weight loss after the isothermal run at 773 K was 36.0 wt %, which was slightly higher than 35.4 wt % but reasonably consistent with the value obtained from the previous run. After the catalyst weight stabilized at 773 K, helium gas was introduced into the furnace chamber to flush out all remaining hydrogen. Air was then introduced at 773 K. The weight gain was 25.5 wt %, slightly lower than the value obtained previously, 26.0 wt %, when the catalyst was

heated from room temperature to 773 K in flowing air. The final weight was 10.5% below the original weight of the sample.

It can be seen that the weight loss was quite negligible after 673 K (Figure 30). Then the optimum temperature for the in-situ catalyst reduction was determined to be 673 K.

The effect of a very fast heating rate on reduction is presented in Figure 31. The sample was heated to the final temperature, 773 K, within 3 minutes. After the catalyst weight stabilized at 35.4 wt % loss, helium and air were introduced into the sample as before (Figure 30). The weight gain after oxidation in air was only 2.5%, compared to the previous 26.0%.

The catalyst sample had to be heated from room temperature to 673 K at a heating rate of 2 K/min and the temperature had to be maintained at 673 K in order to determine a minimum reduction time at 673 K necessary for a complete reduction. This experiment was carried out with a Perkin-Elmer TGA unit due to the limitations of the DuPont TGA 951. The weight loss curve, when the catalyst was heated from room temperature to 673 K at a heating rate of 2.5 K followed by a period in which the temperature was maintained at 673 K is presented in Figure 32. After a sharp weight loss at 673 K the catalyst weight loss became negligible after 2 hours reduction at 673 K. The final weight loss was again 35.4 wt % and the minimum time necessary for a complete reduction was 2 hours at 673 K.

A comparison of weight change between the coprecipitated iron-manganese and a precipitated iron catalyst at the reduction condition is presented in Figure 33. Each catalyst was subjected to

Figure 30

Isothermal Catalyst Reduction Sequence

Coprecipitated Iron-Manganese Catalyst;

Hydrogen/Helium/Air Atmospheres

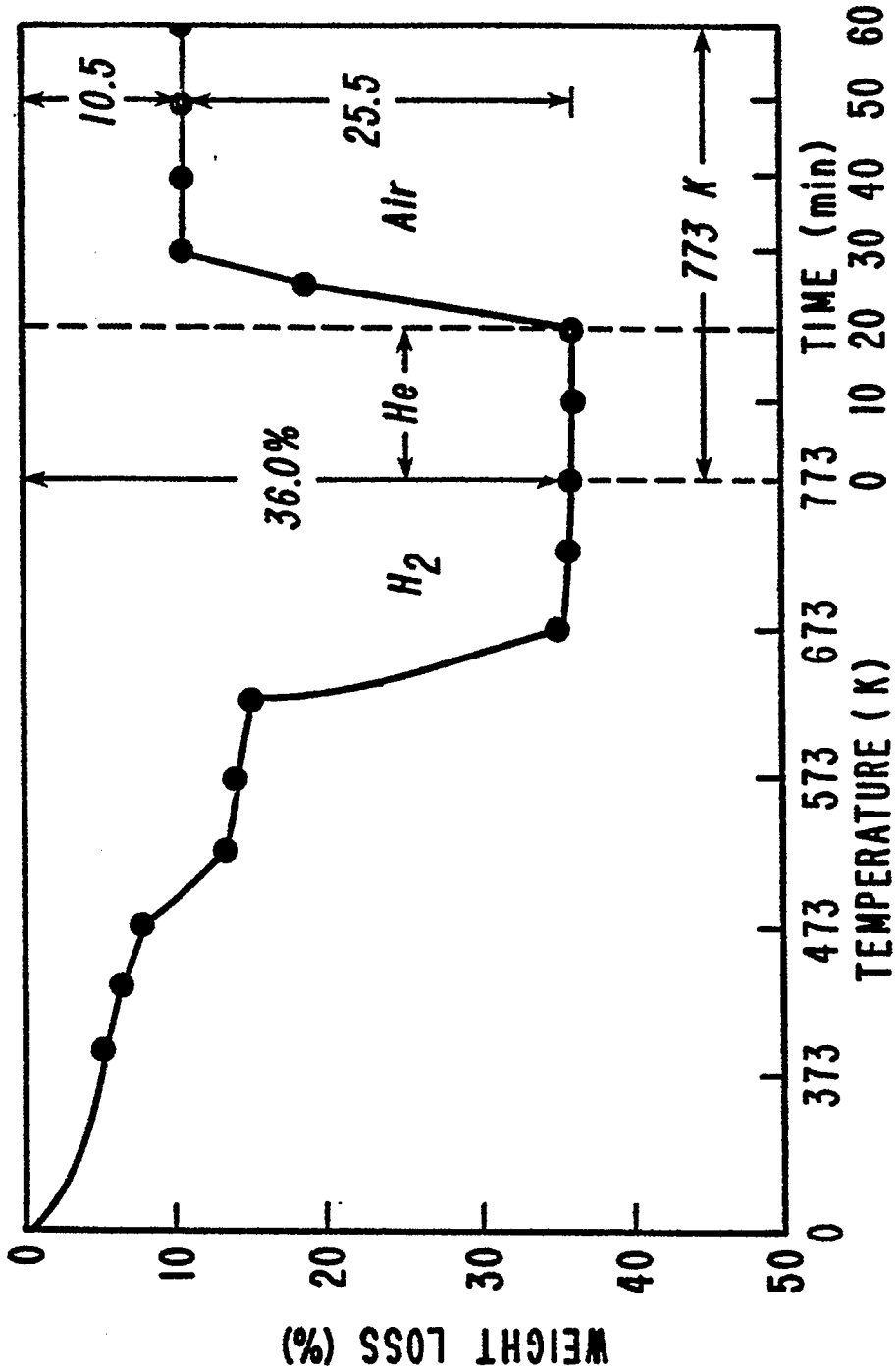
10.5
25.5
Air
773 K
He
36.0%
H2
WEIGHT LOSS (%)
0
10
20
30
40
50
373
473
573
673
773
TEMPERATURE (K)
0
10
20
30
40
50
60
TIME (min)

Figure 31

Effect of Fast Heating Rate on
Catalyst Reduction

Coprecipitated Iron-Manganese Catalyst;

Hydrogen/Helium/Air Atmosphere

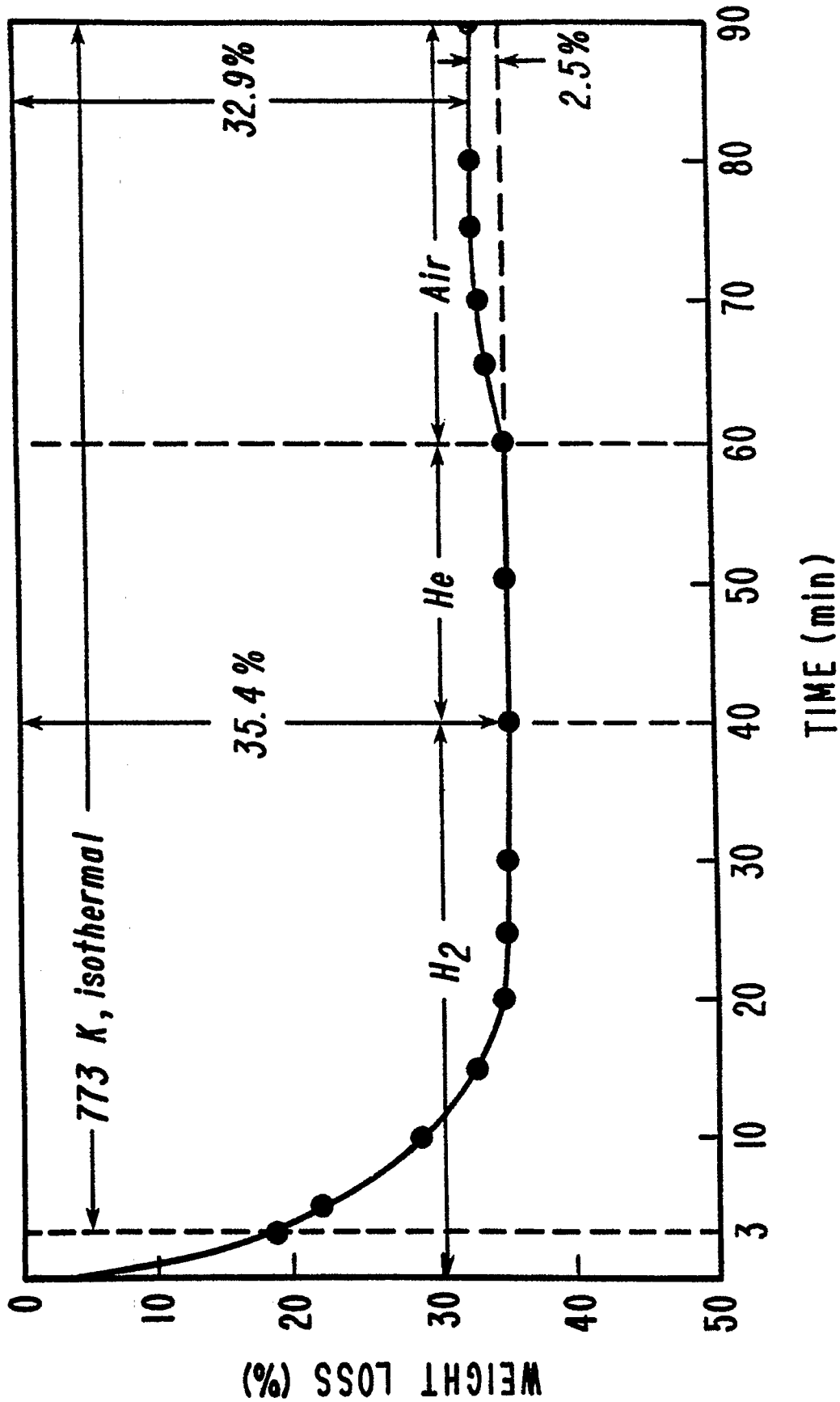
773 K, isothermal
32.9%
35.4 %
2.5%
H2
He
Air
WEIGHT LOSS (%)
TIME (min)
0
10
20
30
40
50
3
10
20
30
40
50
60
70
80
90

Figure 32

Reduction of Coprecipitated Iron-Manganese Catalyst at 673 K

Hydrogen Atmosphere

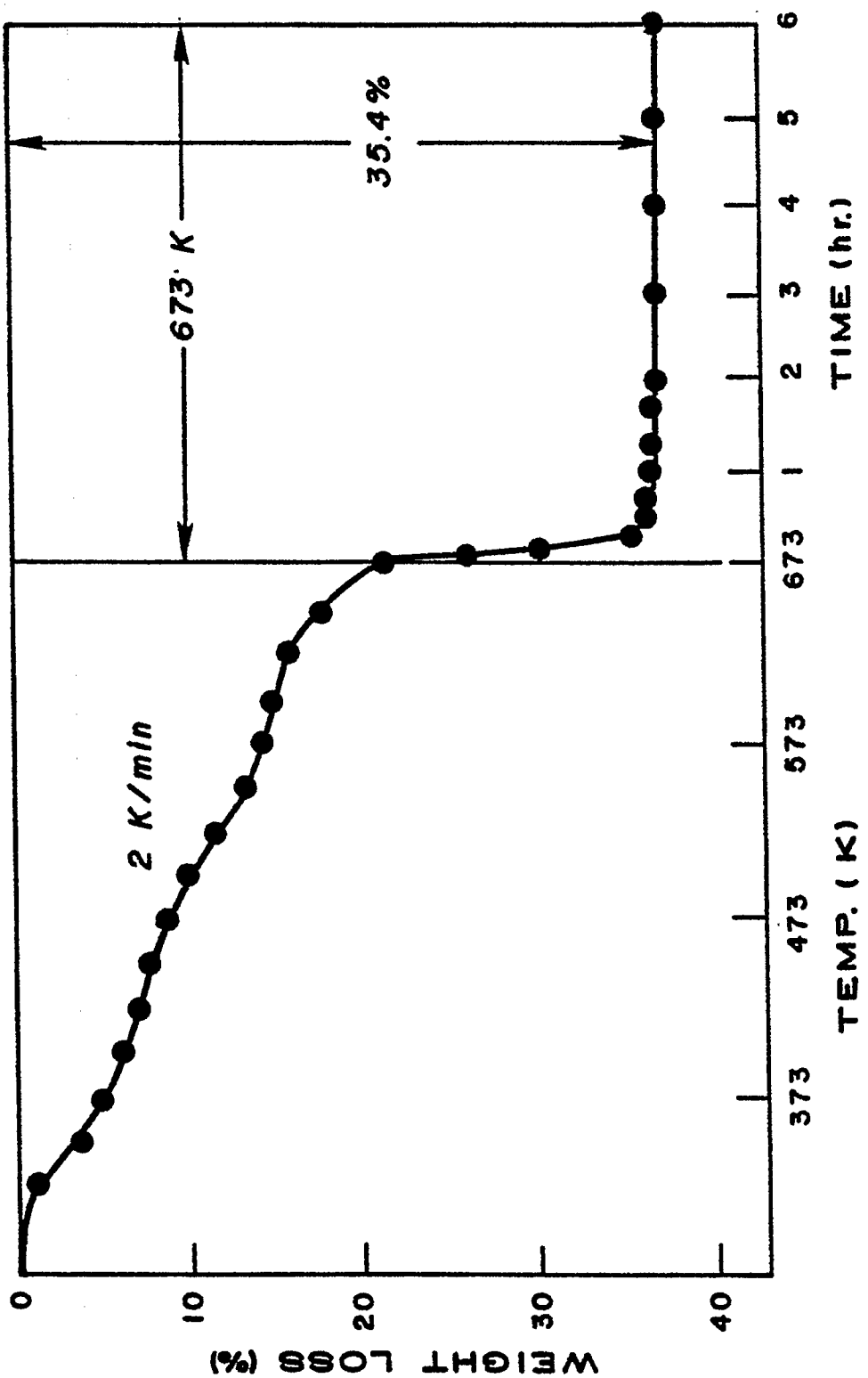
WEIGHT LOSS (%)
0
10
20
30
40
TEMP. (K)
373
473
573
673
TIME (hr.)
1
2
3
4
5
6
2 K/min
673 K
35.4%

Figure 33

Reduction of Precipitated Iron and Coprecipitated Iron-Manganese Catalyst

Hydrogen/Air Atmosphere

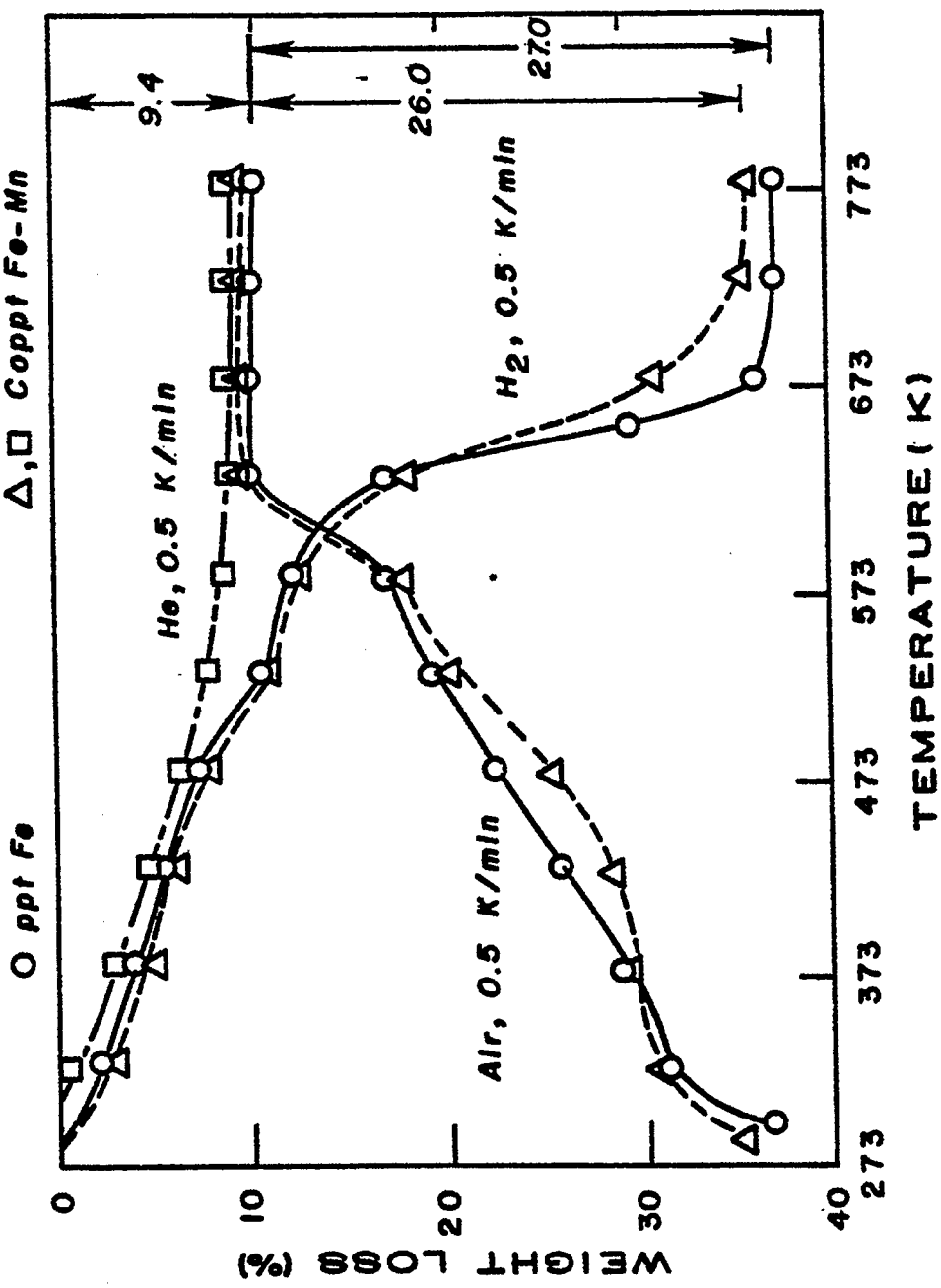
9.4
26.0
27.0
O ppt Fe
Δ,□ Coppt Fe-Mn
He, 0.5 K/min
H2, 0.5 K/min
Air, 0.5 K/min
WEIGHT LOSS (%)
0
10
20
30
40
273
373
473
573
673
773
TEMPERATURE (K)

the same reduction-oxidation cycle. The catalyst was heated from room temperature to 773 K at a heating rate of 0.5 K/min in hydrogen and was cooled to room temperature in flowing hydrogen. Air was introduced and the sample was heated again to 773 K at a heating rate of 0.5 K/min in air. The precipitated iron catalyst lost 36.0 wt % after reduction, slightly higher than 35.4% of coprecipitated iron manganese catalyst, and gained 27.0 wt % after oxidation (Figure 33). This experiment indicated that the two catalysts showed the same behavior under the reduction conditions and the same optimum reduction conditions can be used for the precipitated iron catalyst as well as the coprecipitated iron-manganese catalyst.

Raney Catalyst

A few preliminary reduction studies have been carried out for a Raney iron-manganese catalyst (R-FeMn-A90) with the DuPont TGA. However, an electromagnetic interaction between the Raney catalyst and the TGA furnace caused an apparent weight increase instead of a decrease during the reduction. Therefore, a Perkin-Elmer TGS-2 system was used exclusively for the reduction study of the Raney catalysts. The TGS-2 unit has been proved to be free from such electromagnetic interaction with a ferromagnetic sample, such as the Raney iron or Raney iron-manganese catalyst.

A series of similar experiments was carried out with the Raney catalyst as was done with the precipitated catalyst. The effect of different heating rates during oxidation of a catalyst, which had been reduced in flowing hydrogen before oxidation is shown in Figure 34. Initially, the catalyst had been dried at room

Figure 34

Effect of Heating Rate During Catalyst Oxidation on Weight Gain

Raney Catalyst: R-FeMn-A90;

Hydrogen/Air Atmosphere

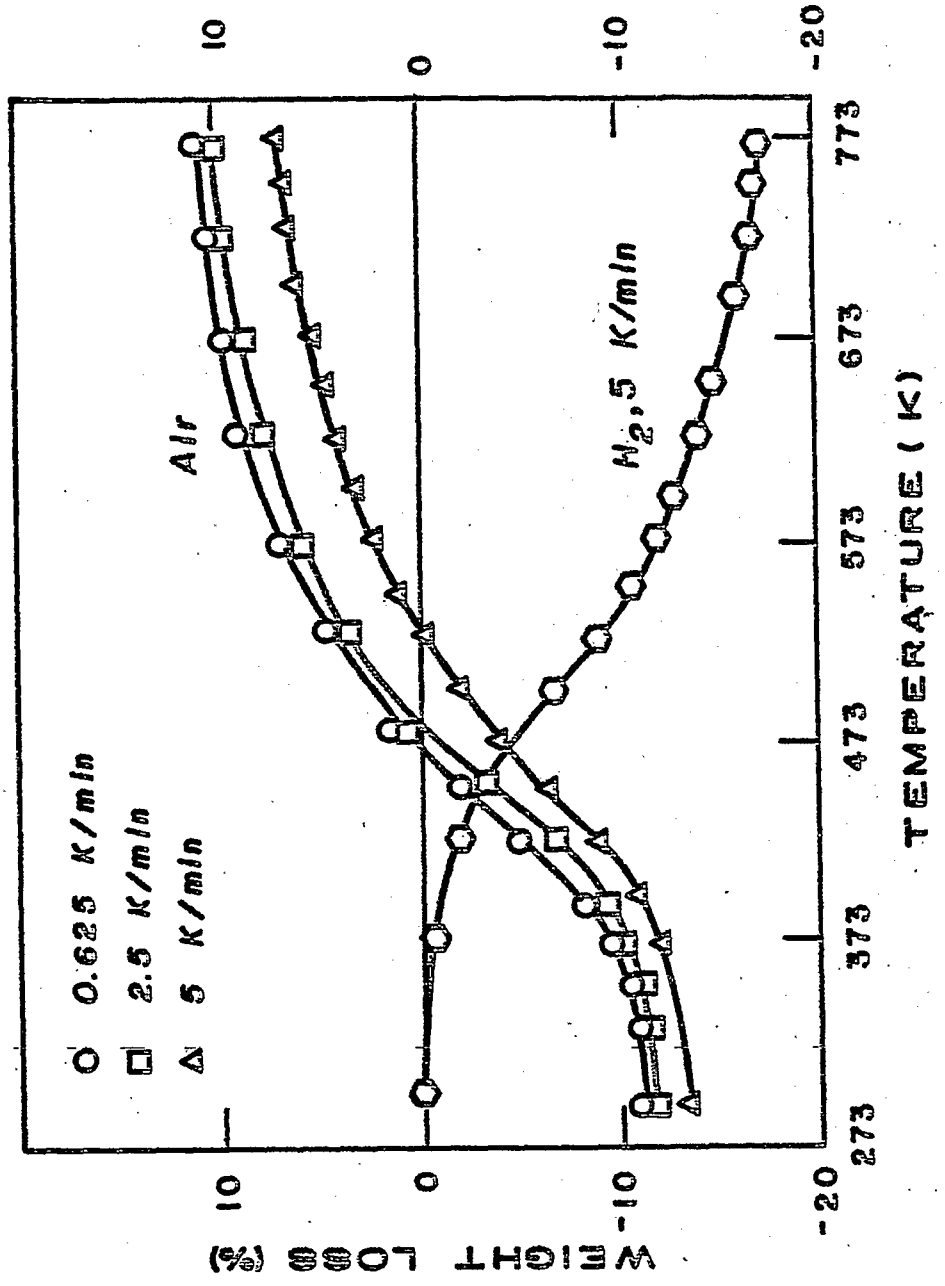
WEIGHT LOSS (%)
10
0
-10
-20
273
373
473
573
673
773
TEMPERATURE (K)
Air
N_2, 5 K/min
0.625 K/min
2.5 K/min
5 K/min

temperature in flowing helium to evaporate ethanol from the catalyst surface. After the catalyst weight stabilized, it was heated to 773 K at a heating rate of 5 K/min in flowing hydrogen. It was then cooled to room temperature and a stream of air was introduced into the furnace chamber. The catalyst weight increased slightly due to oxidation at room temperature. The catalyst was then heated to 773 K in air at three different heating rates, that is, 0.625, 2.5, and 5 K/min. The oxidation of the catalyst at the 0.625 and 2.5 K/min heating rates resulted in a same weight gain of 11.2% over the original weight of the sample. The oxidation at a heating rate of 5 K/min resulted in a smaller weight gain than the oxidation at the lower heating rates, that is, a weight gain of 7.2% over the original weight. Therefore, a heating rate of 2.5 K/min during oxidation was chosen to study the effect of different heating rates during reduction in hydrogen. The effect of different heating rates during the reduction of the catalyst in flowing hydrogen on the subsequent oxidation is shown in Figure 35. The heating rate during oxidation of the catalyst was fixed at 2.5 K/min. Three different heating rates were used during the reduction step, that is, 0.625, 2.5, and 5 K/min. All of the three different heating rates during the reduction resulted in the same weight loss, 16.8 wt % at 773 K. The samples, which had been reduced at the heating rate of 0.625 and 2.5 K/min, gained the same weight, 9.6% above the original weight of the sample after oxidation in air. The sample, which had been reduced at the heating rate of 5 K/min, gained slightly less weight than the above cases, 9.3 wt % above the original weight of the sample. The above

Figure 35

Effect of Heating Rate During Catalyst Reduction on Catalyst Oxidation

Raney Catalyst: R-FeMn-A90;

Hydrogen/Air Atmosphere

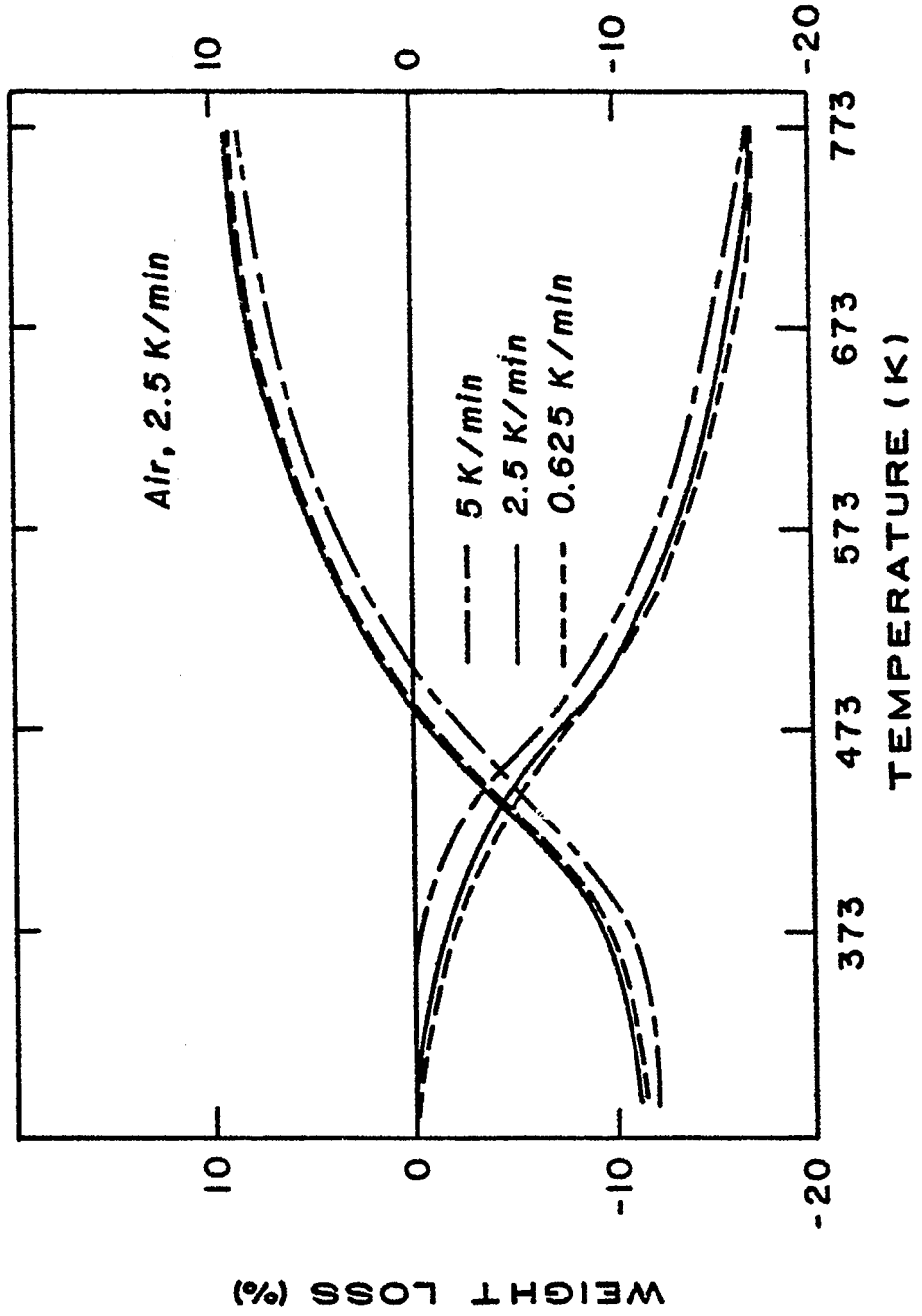
Air, 2.5 K/min
5 K/min
2.5 K/min
0.625 K/min
10
0
-10
-20
373
473
573
673
773
TEMPERATURE (K)
WEIGHT LOSS (%)

results led to the selection of 2.5 K/min as the standard heating rate during reduction.

The Raney iron-manganese catalyst (R-FeMn-A90) was subjected to a series of isothermal reductions to find an optimum temperature for the reduction of the Raney catalysts (Figure 36). Initially, the catalyst was reduced at a low temperature until the catalyst weight stabilized, then the catalyst was heated to the next higher reduction temperature and so on. The temperature was increased in increments of 50 K. The catalyst weight change slowed down after 648 K, although there was a slight weight loss during the reduction between 648 and 773 K. The weight loss at 648 K was 17.52%, while it was 18.60 wt % at 773 K. The temperature 648 K was chosen as the optimum reduction temperature, rather than 773 K, to avoid any adverse effects on catalyst surface area via sintering during a reduction at 773 K. Catalyst activity tests with the precipitated catalysts in a fixed-bed reactor indicated that reduction of the catalyst at 673 K for 5 hours resulted in a significant increase in catalytic activity, when compared to the reduction at 773 K for 24 hours.

Finally, a minimum reduction time necessary for a complete reduction of the Raney catalysts was determined (Figure 37). The catalysts were heated under hydrogen to 648 K at a heating rate of 2.5 K/min and the temperature was maintained at this level. Among the several Raney catalysts tested, the R-FeMn-A90 catalyst took the longest time, 5 hours, until the weight stabilized at 648 K. Therefore, a reduction at 648 K for 5 hours was chosen as a standard reduction condition for all the Raney catalysts, which were to be subjected to a standard activity test in the fixed-bed reactor.

Figure 36

Isothermal Catalyst Reduction Sequence

Raney Catalyst: R-FeMn-A90;

Hydrogen Atmosphere